The Geological Society of America
Special Paper 439
2008

Late Pleistocene lakes and wetlands, Panamint Valley, Inyo County, California

A.S. Jayko*
U.S. Geological Survey, 3000 East Line Street, Bishop, California 93514, USA

R.M. Forester
2364 S. Harlan St., Lakewood, Colorado 80227, USA

D.S. Kaufman
Department of Geology, Northern Arizona University, Box 4099, Flagstaff, Arizona 86011, USA

F.M. Phillips
Department of Earth and Environmental Science, New Mexico Institute of Mining and Technology, 801 Leroy Place, Socorro, New Mexico 87801, USA

J.C. Yount
U.S. Geological Survey, Box 25046, MS 980, Denver, Colorado 80225, USA

J. McGeehin
U.S. Geological Survey, 12201 Sunrise Valley Drive, MS 926A, Reston, Virginia 20192, USA

S.A. Mahan
U.S. Geological Survey, Box 25046, MS 974, Denver, Colorado 80225, USA

ABSTRACT

Pleistocene deposits in Panamint Valley, California, document the changes in pluvial lake level, source water, and elevation of the regional groundwater table associated with climate change. The oxygen isotope stage (OIS) 2 and 6 lacustrine record is well preserved in surficial deposits, whereas the OIS 3–5 lacustrine-paludal and lacustrine record is mainly derived from an archived core sample. Amino acid racemization ratios in ostracodes and gastropods suggest that the shoreline and groundwater-discharge features that lie between ~600 and 550 m elevation formed during one highstand, probably during OIS 6.

A fossiliferous part of the ~100-m-deep core DH-1, which was drilled in the Ballarat Basin during the late 1950s, was resampled in this study. Comparison of DH-1 with core DH-3 from Panamint Valley and core OL-92 from Owens Lake suggests the 34–78-m-depth interval of DH-1 may span all or much of OIS 4. The microfauna from this depth interval indicate a saline marsh or shallow lacustrine environment, but not

*ajayko@usgs.gov

Jayko, A.S., Forester, R.M., Kaufman, D.S., Phillips, F.M., Yount, J.C., McGeehin, J., and Mahan, S.A., 2008, Late Pleistocene lakes and wetlands, Panamint Valley, Inyo County, California, *in* Reheis, M.C., Hershler, R., and Miller, D.M., eds., Late Cenozoic Drainage History of the Southwestern Great Basin and Lower Colorado River Region: Geologic and Biotic Perspectives: Geological Society of America Special Paper 439, p. 151–184, doi: 10.1130/2008.2439(07). For permission to copy, contact editing@geosociety.org.

a large lake. The ostracode assemblage requires low ratios of alkalinity to calcium (alk/Ca) water likely indicative of solutes in deep regional groundwater sources rather than the high alk/Ca solutes common to the Owens River system.

OIS 2–aged sediment from surficial deposits, a shallow auger hole, and core DH-1 contain faunas, including the ostracode *Limnocythere sappaensis,* which require the high alk/Ca evolved solutes common to the Owens River. The elevation of the lacustrine sediments further indicates a moderate-sized saline lake around 180–200 m depth. In the northern Lake Hill basin, a saline lake persisted until at least 16 ka, and it was succeeded by fresh, groundwater-supported wetlands, which were fully developed by ca. 12,575 ^{14}C yr B.P. and which persisted until around 10,500 ^{14}C yr B.P., when the basin became a dry playa.

Keywords: Panamint Valley, Owens River System, Pleistocene glacial lakes, Gale strandline, LGM eastern Sierra region, hydrochemisty saline lake.

INTRODUCTION

The Pleistocene stratigraphic record from Searles, Owens, and Death Valleys in the southwest Great Basin area has provided a framework for understanding the regional climate history and landforms in Panamint Valley (Stuiver, 1964; Smith et al., 1983; Smith and Bischoff, 1997; Lowenstein et al., 1999; Forester et al., 2005). This paper summarizes chronostratigraphic and paleoecologic investigations of late Pleistocene beach, wetland, and lacustrine deposits in Panamint Valley. In addition, we provide a summary of new data obtained from core material that was archived in the 1950s (Smith and Pratt, 1957). These new observations help to constrain the elevation of shorelines during the Last Glacial Maximum (LGM) and the sources of water and duration of lakes in Panamint Valley during the late Pleistocene.

In 2001, four tufa samples from elevations of 357 m to ~512 m yielded Last Glacial Maximum ages of ca. 15,050–22,600 ^{14}C yr B.P. (Jayko et al., 2001). This was the first indication that the oxygen isotope stage (OIS) 2 lake in Panamint Valley may have been quite large (Jayko et al., 2001) and its shorelines were significantly higher than the ~383 m elevation reported by R.S.U. Smith (1976). These results prompted additional sampling of marls and silt for microfauna—in particular, for analysis of ostracode paleoenvironmental indicators. Aquatic gastropods were collected for amino acid racemization analysis (AAR) with the objective of determining the relative age and timing of lacustrine events.

Fundamental differences in the solute chemistries of the water sources that intermittently occupied Panamint Valley also help to establish the Pleistocene chronostratigraphy in the absence of robust dates using U-series, ^{36}Cl, IRSL (infrared stimulated luminescence), and TL (thermoluminescence) methods. These different water sources, the dominance of which is climate dependent, differ in major- and trace-element chemistries, which make possible their differentiation by faunal paleoenvironmental proxies and by trace-element geochemistry. Our results suggest that Panamint Valley lakes and wetlands were supported by Owens River–derived surface water during glacial-pluvial cycles. During drier episodes, springs and wetlands or shallow lakes were supported by flow from local spring and deep aquifer sources.

Basin Setting

Panamint Valley is one of a continuous chain of basins linked by the Owens River system during glacial and pluvial periods (Russell, 1885; Campbell, 1902; Gale, 1914a, 1914b; Blackwelder, 1933, and subsequent work). The valley occupies a topographic depression with the Owens Valley and associated drainages to the west and Death Valley to the east (Fig. 1). The valley floor lies at 317 m, ~610–795 m lower than the Owens Valley playa and ~370 m higher than Death Valley. Panamint Valley is rimmed by 2000 to 2600 m ranges to the west and by the Panamint Range to the east, which generally lies between 2000 and 2700 m, but reaches 3365 m at Telescope Peak. The mean annual temperature of the valley is ~18 °C, and mean annual rainfall is ~90 mm/yr.

Panamint Valley contains two basins floored by playa surfaces at ~470 m and 317 m elevation separated by a divide that is presently at ~521 m elevation. The northern, smaller, and higher basin is here referred to as the Lake Hill basin, and the prominent southern one is called the Ballarat basin (Fig. 1). The Owens River system reaches the south end of Panamint Valley through streamflow when Searles Valley fills to its external spillway level at 690 m elevation (Gale, 1914b). The Owens River system in turn continues to Death Valley via Wingate Wash when the Panamint Valley fills to ~602 m elevation (Gale, 1914b; Blackwelder, 1933; Smith, 1976).

The regional topographic gradient of the valley floors, and likely the principal hydrographic gradient, is eastward. An eastward slope of the groundwater table surface has been documented in well data from the Indian Wells Basin (Fig. 1) and adjacent areas that lie west and southwest of Panamint Valley (Kunkel, 1962). Although the regional gradient slopes eastward from the hydrologic head provided by the high Sierra Nevada Range to the

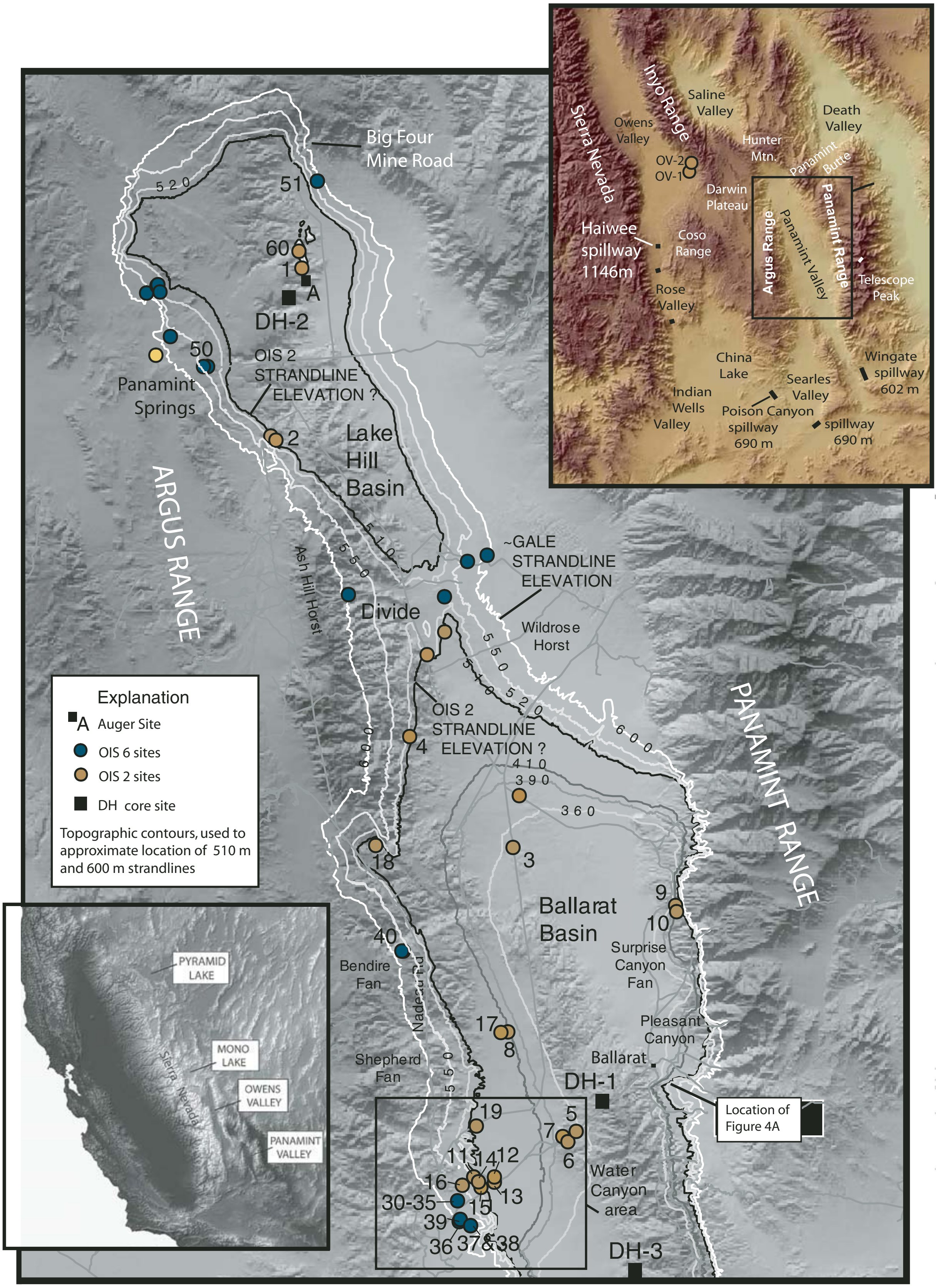

Figure 1. Location of tufa sites; sampled sites are numbered. Inset maps show two amino acid racemization (AAR) samples from Owens Valley, location of basins in the Owens River system, and the eastern Sierra Nevada region. Topographic contours representing approximate location of oxygen isotope stage (OIS) 2 and OIS 6 highstands are noted.

west, some groundwater recharge is also provided by runoff from the central Panamint Range.

Panamint Valley is arid, and playa surfaces receive sporadic runoff from local watersheds. Shallow auger holes indicate that the water table presently lies ~1–3 m deep under the Ballarat playa in the southern basin (Carranza, 1965; Jayko et al., 2002). Several of the canyons that drain the central part of the Panamint Range support perennial runoff. Springs and seeps are also present at the toes of fans that emanate from these canyons and discharge onto the northeast side of the Ballarat playa.

Panamint Valley is one of several large tectonically active grabens that lie within the eastern Sierra Nevada region. The valley lies in a zone of active transtensive deformation associated with oblique strike-slip deformation along part of the North America–Pacific plate boundary (cf. Reheis and Sawyer, 1997). The regional tectonic setting strongly influences the active hydrothermal and structural characteristics of the region. Thermal springs are associated with large basin-bounding faults in the Coso Range and in Owens, Saline, Panamint, Fish Lake, and Death Valleys. Many of the active faults in the region tap into geothermal aquifers. Warm springs discharge along the base of the fault-controlled range front adjacent to the central part of the Panamint Range, indicating groundwater discharge from a deeper, geothermal source.

Water Sources

Ostracode assemblages indicate that two significantly different source-water chemistries have alternately dominated the basins in Panamint Valley. These water chemistries can be attributed to geological differences in the flow path of the Owens River versus the flow path of groundwater that is likely deep-sourced and includes fracture-controlled interbasin flow. Different water sources indicative of local as well as surface overland flow have previously been inferred from Sr isotope geochemistry and rare earth elements (Smith et al., 1998; Pretti and Stewart, 2002; Stewart, 1998).

The surface flow of the Owens River system traverses significant igneous rock, including the Bishop Tuff in the upper part of its watershed, Sierran granitic rocks throughout, and the bimodal Coso volcanic field in the south. These geologic domains are dominated by Cenozoic and Mesozoic rock with rock chemistries that are high in silica and relatively alkalic and that have low $^{87}Sr/^{86}Sr$ isotopic ratios. For example, the $^{87}Sr/^{86}Sr$ of Bishop Tuff is ~0.7078 (McConnell, 1994), Sierran intrusive rocks range from ~0.704 to 0.706 (Kistler and Peterman, 1973; 1978), and Coso volcanic rocks range from 0.7033 to 0.7038 (Groves, 1996). Similar low isotopic ratios are found in the shell remains, minerals, and tufa that precipitate when Owens River surface water dominates the Panamint Valley (Stewart, 1998). The siliceous alkaline rocks of the Owens River watershed tend to produce high solute ratios of alkalinity to calcium (alk/Ca) in the surface water.

In contrast to Owens River–derived water, the Panamint Valley groundwater has a low alk/Ca ratio. The flow path for the groundwater generally traverses isotopically evolved bedrock and marine sedimentary rock (evolved with respect to chondrites), which consist of abundant Paleozoic carbonate lithologies and Precambrian metasediment. Bedrock in the Panamint Range (Wasserburg et al., 1964) and in the nearby region (DePaolo, 1981; Domenick et al., 1983) has enriched $^{87}Sr/^{86}Sr$, ranging between 0.7115 and 0.8040. Thus, groundwater flowing through the continental bedrock is likely to have high $^{87}Sr/^{86}Sr$, compared to the Owens River surface path, which traverses abundant siliceous, less isotopically evolved rock. Stewart et al. (2001) found $^{87}Sr/^{86}Sr$ values of 0.7098–0.7104 from the highstand tufas in Panamint Valley and 0.7159 from sulfate in the Panamint core DH-3 drilled to the south of DH-1 in the basin depocenter. These results support the interpretation that overflow from the Owens River system produced the large lakes in Panamint Valley and that another water source, likely part of a deep aquifer, supported the lake in which the sulfates were deposited.

Both the Sr isotope geochemistry reported by earlier workers and the faunal data from this study are used to indicate the presence or absence of Owens River flow into the Panamint Valley. Carbonate sediments from Owens Lake core OL-92 also contain Sr isotope ratios that range between 0.7091 and 0.7093 over the last 25 k.y. (Stewart, 1998). In contrast, $^{87}Sr/^{86}Sr$ ratios from Death Valley core DV93–1 range between 0.7132 and 0.7152 in sediments spanning the last ~100 k.y. (Sr isotope data from Z. Peterman, U.S. Geological Survey, written commun.).

Previous Work

Pleistocene lacustrine features have been recognized in the eastern Sierra and surrounding region since the late 1800s and early 1900s (Russell, 1885; Gilbert, 1890; Gale, 1914a, 1914b). Lacustrine or wetlands gastropods were first reported in deposits on the west side of Panamint Valley by Gale (1914b). Hanna (1963) described additional gastropod localities from the highstand deposits. Planktonic microfossils associated with diatomite deposits were reported during exploration for economically viable evaporite deposits by American Potash and Chemical Company in the 1950s (Wornardt, 1964).

R.S.U. Smith (1976) undertook the most detailed mapping of lacustrine surficial features in Panamint Valley. Smith's thorough work concentrated on the highstands of the lake that occupied elevations of 580–610 m and 341–385 m. He also recognized intermediate stands and low-elevation strandlines, but these were given less attention. In addition to establishing a record of the highstand features that ring the basin, including tufa, beach gravels, and molluskan assemblages, Smith documented late Pleistocene tectonic deformation of the highstand shorelines. Smith (1976, 1978) also reported numerous fossil localities in the basin and named the ~600 m strandline after Gale, who first described it in the literature (Gale, 1914b). The highstand of the lake in Panamint Valley is controlled by a spillway to Death Valley at the head of Wingate Wash (Fig. 1). The age and correlation of the lower-elevation strandlines and their relation to late Pleistocene pluvial events are unknown. Several different methods have been used in attempts to date surficial and core deposits in Panamint Valley over the past 20 yr.

U-series dating of highstand nearshore and spring-mound tufa has yielded isochron ages between 54 and 91 ka (Fitzpatrick and Bischoff, 1993). Tufa from Ash Hill gave 68 ± 25 ka at 536 m elevation, with $R^2 = 0.848$; marl in Water Wash gave 66 ± 9 ka at 603 m, with $R^2 = 0.960$, and 54 ± 8 ka at 603 m, with $R^2 = 0.927$; Revenue Canyon tufa gave 91 ± 5 ka at 618 m, with $R^2 = 0.997$; and one gastropod-bearing marl gave 24 ± 12 ka at 579 m from Bendire Canyon, but it had a low R^2 (= 0.432; Fitzpatrick and Bischoff, 1993). The results suggest that the system was open with respect to uranium, and therefore the ages were considered not to be indicative of the depositional age and not reliable (Fitzpatrick and Bischoff, 1993).

Chlorine-36 dating has also been applied to boulders and tufa lying on shorelines inset on alluvial fans. The ^{36}Cl exposure ages on tufa and boulders from the Gale-stage shoreline at Pleasant Canyon were 100–150 ka at ~610 m elevation, suggesting an OIS 6 age. Tufa gave exposure ages of 70–80 and 84–100 ka for the ~580 m shoreline on Ash Hill (Phillips and Zreda, 1999); these are most likely minimum ages, also suggesting an OIS 6 age for the highstand.

Salt deposits recovered from Panamint drill-hole 3 (DH-3) core (Smith and Pratt, 1957), drilled near the depocenter in the southern part of the southern playa (Fig. 1), also indicate an open geochemical system with respect to uranium and thorium (Fitzpatrick et al., 1993). The U-series results show large variation and some age reversal down section, but in spite of that, they may provide approximate age ranges for successive 15–25 m sections (Fig. 2) (Fitzpatrick et al., 1993). Chlorine-36 dating of salt from three horizons in DH-3 (Jannik et al., 1991), two of which are within the depth interval shown in Figure 2, yielded significantly older ages than the U-series results by ~60 to 100 k.y. and identical results at different depths (Fig. 2). In summary, the radiometric techniques have provided general constraints for the basin evolution, but reversals, large age ranges in short stratigraphic intervals, and large analytical errors plague the results (Fitzpatrick and Bischoff, 1993; Fitzpatrick et al., 1993; Jannik et al., 1991).

OBJECTIVES AND METHODS

Numerous strandline features are found over a nearly 300-m-elevation range in Panamint Valley from just above the playa floor to the spillway at Wingate Wash. Establishing whether these features are the record of a single large recessional lake event or multiple lacustrine events is a first step toward understanding the evolution and rates of surface and tectonic processes in the basin. Although significant work documenting the location and deformation of the highstand strandlines has been completed (R.S.U. Smith, 1976), the age and correlation of many intermediate strandlines remain uncertain.

This study of late Pleistocene lakes was undertaken during a regional, 1:100,000-scale effort to map surficial deposits of the Darwin Hills 30′ × 60′ quadrangle (Jayko, 2008). Many localities with lacustrine deposits have been noted by previous workers, including: (1) south of Water Canyon at ~610 m elevation (Smith, 1976; Fitzpatrick and Bischoff, 1993; Stewart, 1998), (2) northern end of Ash Hill at about ~520 m (Hall and MacKevett, 1962; Smith, 1976; Fitzpatrick and Bischoff, 1993), (3) east of Panamint Springs at ~550 m (Hall and MacKevett, 1962; Smith, 1976) and Lake Hill at ~470 m (Davis, 1970), and (4) Big Four Mine road (Davis, 1970; Smith, 1976). Localities described in previous work, including Hanna (1963), Wornardt (1964), Davis (1970), Smith (1976), and Hall and MacKevett (1962), were resampled.

Lacustrine and wetlands deposits were sampled from late Pleistocene beach and nearshore deposits for macro- and microfaunal assemblages. Tufa, marls, and gastropods were collected to constrain the age, duration, and characteristics of the water bodies that occupied Panamint Valley. Emphasis was directed toward sampling from intermediate and lowstand shoreline and nearshore deposits in an effort to establish the elevation of the Last Glacial Maximum lake in Panamint Valley.

The ^{14}C dating method was used to identify deposits potentially formed during OIS 2. Uncorrected IRSL and TL ages on silt associated with marl-bearing wetland and lacustrine deposits and ^{36}Cl ages on tufa provided minimum ages for some deposits at intermediate elevations. Reexamination of the fossil-bearing archived core extracted by Smith and Pratt (1957) provided paleoenvironmental information constrained by two ^{14}C ages near the top of the core. The DH-1 core was also sampled for amino acid racemization (AAR) on ostracodes and ostracode identification. The initial objective was to use the ostracode AAR ratios in the core to correlate to strandline deposits.

^{14}C Dating

Charophyte and other algal tufa samples collected from shallow, nearshore lacustrine and wetlands deposits were acid etched prior to analysis. Most of the surface tufa samples were selected in the field for optimum freshness indicated by good preservation of biogenic characteristics and minimal solution features; however, some amount of weathering, solution, and reprecipitation was evident in most samples. Ostracode samples were considered too small for pretreatment and were processed as is. Plant material was given an acid-alkali-acid (AAA) pretreatment to remove carbonate and humic acid contaminants.

Radiocarbon analyses for this study were performed using liquid scintillation (radiometric) and accelerator mass spectrometry (AMS) techniques. Radiometric samples were processed with benzene and analyzed for ^{14}C activity using liquid scintillation counters at Beta Analytic, Inc., in Miami, Florida. AMS samples were processed to pure carbon (in the form of graphite) at the U.S. Geological Survey (USGS) Radiocarbon Laboratory in Reston, Virginia. AMS dating was carried out at the Center for Accelerator Mass Spectrometry (CAMS), Lawrence Livermore National Laboratory, Livermore, California. The bulk-rock tufa samples were dated by Beta Analytic. Subsurface samples from a

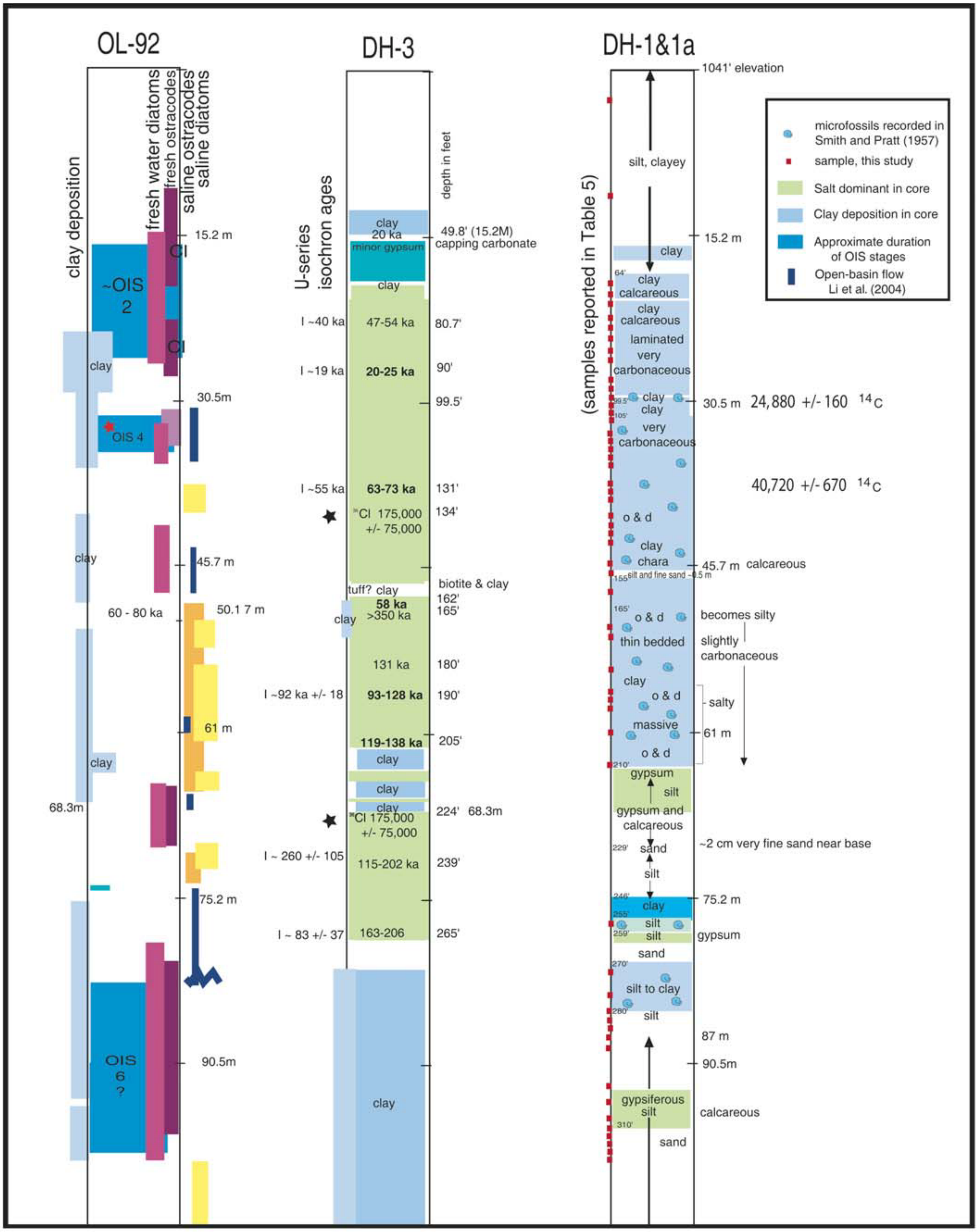

Figure 2. Summary of lithologic variation, ages, and faunal control from Owens Lake core OL-92 and Panamint cores DH-1&1a and DH-3. All three cores are scaled the same in meters (feet also shown for reference). OL-92—Owens core data summarized from Smith and Bischoff (1997); depth of clay deposition is noted on left of column; depths of fresh versus saline diatom and ostracode assemblages are shown on right of column. Approximate depth to oxygen isotope stage (OIS) is also shown. Timing of Owens Lake open-basin conditions in OL-92 core (dark blue bars) is from Li et al. (2004). Results from previous dating of DH-3 core: U-series isochrons on left of DH-3 column and whole-rock U-series inside DH-3 column (Fitzpatrick and Bischoff, 1993); depth in feet is on right of column. Meteoric ^{36}Cl ages from Jannik et al. (1991) are noted with black star on DH-3.

4 m auger, the archived DH-1 core, and one stromatolitic tufa sample yielded small volumes of handpicked material that were analyzed using AMS.

Quoted ^{14}C ages in this study are in radiocarbon years using the Libby half-life of 5568 yr and are normalized to a common $\delta^{13}C$ of −25‰, following the conventions of Stuiver and Polach (1977). Actual $\delta^{13}C$ values were measured for individual samples when possible. These data are given in Tables 1A and 1B. Measured $\delta^{13}C$ values are shown with one decimal place. Samples that were not measured for $\delta^{13}C$ are shown as estimates without a decimal place. Estimates are based on expected $\delta^{13}C$ values for similar sample material.

We have not established a reservoir effect for this basin, and little has been reported about this potential error for nearby basins

TABLE 1A. RADIOCARBON DATES ON SHELL AND TUFA IN SURFICIAL DEPOSITS FROM PANAMINT VALLEY

Site, Fig. 1	Sample location and elevation (m, ft)	Conventional radiocarbon date* (yr B.P.)	$\delta^{13}C$ (‰)	Calibrated date† (cal yr B.P.)	Depositional environment
1	475 (1560)	11,880 ± 70	–2.3	13,920–13,570	Reefal tufa with encased gastropods on Lake Hill bedrock
2	500 (1640)	14,950 ± 80	+3.5	18,580–17,990	Very large tufa mound on bedrock
3	357 (1170)	15,050 ± 80	+2.2	18,640–18,060	Rhizoliths associated with “popcorn”-type tufa characteristic of spring discharge
5	372 (1220)	20,190 ± 130	–2.8	24,500–23,840	Lacustrine, nearshore, subwave base, adjacent to wave-cut abrasion surface with beach lag pebbles
6	384 (1260)	17,980 ± 100	+2.2	21,770–20,830	Bedded, interbedded fine-grained sandstone and silty marl; sample is marl, lacustrine?
7	384 (1260)	21,110 ± 160		25,060–24,690§	Lacustrine, nearshore, subwave base, adjacent to wave-cut abrasion surface with beach lag pebbles
8	415 (1360)	17,130 ± 100		20,500–19,990	Lacustrine marl overlies brecciated spring-mound-like tufa (dated material)
9	415 (1360)	14,150 ± 80		17,310–16,440	Coarse cobble beach, lake transgressed above this elevation at time of stromatolite growth
10	415 (1360)	22,570 ± 110	–22.1	26,690–26,440§	Coarse cobble beach, lake transgressed above this elevation at time of stromatolite growth
11	500 (1640)	28,710 ± 320	–26.1	33,890–33,180§	Massive tufa, locally oxidized; hydrothermally altered?
12	503 (1650)	13,980 ± 80	–25.4	17,050–16,250	Lacustrine, nearshore, subwave base, adjacent to wave-cut abrasion surface with beach lag pebbles
13	506 (1660)	14,130 ± 90	–23.9	17,300–16,400	Lacustrine, nearshore, subwave base, adjacent to wave-cut abrasion surface with beach lag pebbles
14	512 (1680)	18,020 ± 110	–25.4	21,880–20,890	Fringing reefal-like algal tufa overlain by beach gravel
15	512 (1680)	22,600 ± 130	–25.2	26,750–26,450§	Fringing reefal-like algal tufa overlain by beach gravel
4	518 (1700)	17,340 ± 90	–25.1	20,840–20,190	Tufa clast, located above slope break and wave-cut trimline, inferred to be relict lag clast from wetland/spring environment
16	561 (1820)	32,550 ± 270	–24.7	38,100–37,500§	Nearshore deposit overlying abrasion surface. Age considered finite, or reset

Note: Samples 1 and 2, which are from Lake Hill basin, are listed in order of ascending elevation; samples 3 to 16, which are from Ballarat basin, are listed by ascending elevation.

*Radiocarbon date ±1σ using Libby half-life of 5568 yr, Beta Analytic.

†Radiocarbon date calibrated at ±2σ using CALIB v 5.0.2 program (Stuiver and Reimer, 1993) with the INTCAL04 data set (Reimer et al., 2004).

§Conventional radiocarbon date calibrated (cal yr B.P.) after Bard et al. (1998).

TABLE 1B. ACCELERATOR MASS SPECTROMETRY (AMS) RADIOCARBON DATES ON SHELL AND BIOGENIC MATERIAL FROM SUBSURFACE SAMPLES IN PANAMINT VALLEY

Site Fig. 1	Sample number, material dated	Sample location and elevation (m, ft)	Conventional radiocarbon date* (yr B.P.)	Depositional environment
Auger	308–316 cm depth gastropods	468 (1536)	12,575 ± 40	Base of black mat, transition from lake to spring
Auger	402 cm depth ostracodes	466 (1528)	16,735 ± 50	Lacustrine
DH-1	DH-1, 99' depth plant material	286 (941)	24,880 ± 160	Wetlands
DH-1	DH-1, 128–131' depth ostracodes	277 (911)	40,710 ± 760	Wetlands

Note: ^{14}C ages were determined at the Center for Accelerator Mass Spectrometry (CAMS), Lawrence Livermore National Laboratory, Livermore, California.
*Radiocarbon date ±1σ using Libby half-life of 5568 yr.

(Benson et al., 2003; Hajdas et al., 2004), although the effect is described for Owens Lake (Benson et al., 2003). The reservoir effect generally causes ^{14}C ages to be a few hundred to a few thousand years too old because it takes time for atmospheric CO_2 to completely exchange with lakes containing high concentrations of dissolved carbonates. The ^{14}C input equilibrium may be achieved by exchange with atmospheric CO_2 at the lake surface, whereas the inorganic carbon component derives from total dissolved solids (TDS) in groundwater and runoff (cf. Geyh et al., 1998).

The reservoir effect is greatest (worst) when the lake is saline and smallest when the lake is fresh because of the relation between TDS and concentration of dissolved bicarbonate and carbonate content of the lake water. Radiocarbon dates from the ostracode *Limnocythere sappaensis* will therefore represent the highest reservoir effect. In addition to the reservoir effect common to sodium bicarbonate–carbonate lakes, the "age" of dissolved inorganic carbon (DIC) can also be impacted by dead carbon derived from dissolved limestone. Charophytes obtain their photosynthetic carbon from the inorganic carbon rather than the free CO_2 fraction (McConnaughey, 1991), so a ^{14}C age from charophyte tufa will reflect the lake's carbon reservoir, as will ^{14}C ages from ostracode shells.

Both Mono and Pyramid Lakes lie to the north of Panamint Valley, west of the rain shadow generated by the Sierra Nevada Range and along the west side of the Great Basin. The reservoir effect at Pyramid Lake is considered either negligible or 600 yr at the time of the ca. 28 ka Mono Lake magnetic excursion (Benson et al., 2003a). This makes the reservoir effect in Owens Lake either ~450 or ~1050 yr at ca. 28 ka during the Mono Lake excursion (Benson et al., 2003b) because the age control for the excursion is constrained by ^{14}C ages at Pyramid Lake. The reservoir effect appears to be negligible or absent in Mono Lake at that time (Benson et al., 1998, 2003b; Benson, 2006, written commun.). In the absence of constraining reservoir-effect data for Panamint Valley, we report the conventional ^{14}C ages here (Tables 1A and 1B) following other workers in the Mojave area (cf. Wells et al., 2003; Anderson and Wells, 2003).

Amino Acid Racemization

The principles and applications of amino acid racemization (AAR) have recently been reviewed by Wehmiller and Miller (2000). After synthesis by an organism, proteins and their constituent amino acids degrade through a complex series of biogeochemical reactions. The extent to which these reactions have progressed in a fossil is proportional to the length of time elapsed since the organism lived and to the ambient temperature of the reaction medium. The most geochronologically reliable of the complex network of diagenetic reactions is AAR, which involves the interconversion of L-amino acids to their D-isomeric configurations. Most living organisms use amino acids exclusively in the L-configuration. Upon death and removal of biologic constraints, the L-amino acids begin to racemize to their D-configuration. The abundance of D relative to L forms (D/L) defines the extent of racemization for a particular amino acid. The ratio increases with time and temperature until the rate of formation of D-amino acids is compensated by the reverse reaction, and the ratio reaches an equilibrium value of 1.0. In this study, we focus on the D/L values of aspartic acid (Asp) and glutamic acid (Glu).

The analytical procedure used in this study was presented previously in Kaufman and Manley (1998; modified by Kaufman, 2000). Shells were cleaned using standard procedures and hydrolyzed individually in separate microreaction vials by dissolving in 6 *M* HCl, sealing under N_2, and heating at 110 °C for 6 h. The high performance liquid chromatograph analysis employed precolumn derivatization with o-phthaldialdehyde together with the chiral thiol, N-isobutyryl-L-cysteine, to yield fluorescent diastereomeric derivatives of chiral amino acids. The derivatization was performed online prior to each injection using an autoinjector. Separation was by a reverse-phase column packed with a

C_{18} stationary phase using a linear gradient of aqueous sodium acetate, methanol, and acetonitrile. Detection was by fluorescence. Each single-shell subsample was injected once.

We analyzed D/L values for 17 monospecific samples of ostracodes and gastropods from 10 sites in Panamint Valley and for eight samples from four sites in Owens Valley (Table 2). Each sample was composed of 6–21 individual valves (average = 11; more for ostracode samples than for gastropods). Some samples included individual shells with D/L values that were much different than the others of the group. Subsamples with D/L values beyond $\pm 2\sigma$ of the mean of the rest of the group were excluded from the calculations. Of the 275 subsamples analyzed in this study, 27 (9.8%) were rejected. Following data screening, the intervalve variability in Asp and Glu averaged 6% and 7%, respectively, for the 25 samples (the standard errors of the mean were considerably lower). This intershell variation is less than that typically reported for single-age populations of mollusks (Miller and Brigham-Grette, 1989) and ostracodes (Kaufman, 2003a, 2003b), and it attests to the integrity of the samples for amino acid analysis.

Chlorine-36

Chlorine-36 surface-exposure dating is one of a family of terrestrial cosmogenic nuclide (TCN) dating methods (Gosse and Phillips, 2001). These methods rely on the accumulation of rare nuclides that are produced in rocks by the action of galactic cosmic radiation. Chlorine-36 is produced by high-energy neutron reactions (spallation reactions) on the nuclei of K and Ca atoms and by low-energy neutron (thermal and epithermal) absorption reactions by the nucleus of Cl. Given the high Ca concentration of tufa, it is in principle a quite suitable material for ^{36}Cl surface-exposure dating. The half-life of ^{36}Cl is 301,000 ± 4000 yr. Gosse and Phillips (2001) provided a comprehensive description of ^{36}Cl surface-exposure dating and the methodology for its application.

Samples of tufa were collected from outcrops, ground to fine sand size, and leached in deionized water to remove any adsorbed meteoric ^{36}Cl or ^{36}Cl fallout from nuclear weapons testing. This leaching should also have removed any chloride-containing dissolved or particulate salts that might have infiltrated the tufa during exposure on the outcrop. Masses of the sample material,

TABLE 2. RESULTS OF AMINO ACID ANALYSES ON OSTRACODES AND GASTROPODS, PANAMINT AND OWENS VALLEYS

Map site #	Field ID	Age* (ka) or elevation (m)	Taxon	n†	Asp D/L ex§	avg	±1σ	Glu D/L avg	±1σ
Panamint ostracodes older than OIS 2									
Core	DH-1 131–134	>41 ka	*Candona patzucuaro*	17	1	0.422	0.010	0.127	0.008
Core	DH-1 131–134	>41 ka	*Cyprideis beaconensis*	16	0	0.403	0.006	0.116	0.006
Core	DH-1 191–194	–	*Candona patzucuaro*	20	1	0.477	0.008	0.163	0.007
Core	DH-1 191–194	–	*Cyprideis beaconensis*	14	1	0.451	0.005	0.143	0.004
33	181-02	564 m	*Candona*	11	2	0.490	0.038	0.405	0.052
51	193-02	597 m	*Candona*	13	3	0.563	0.050	0.520	0.068
Panamint gastropods older than OIS 2									
51	193-02	597 m	*Helisoma*	9	1	0.760	0.057	0.692	0.047
51	193-02	597 m	*Amnicola*	9	3	0.776	0.049	0.754	0.036
38	189-02	604 m	*Amnicola*	10	0	0.734	0.058	0.735	0.078
38	189-02	604 m	*Valvata*	8	1	0.690	0.058	0.663	0.033
33	181-02	564 m	*Helisoma*	9	1	0.702	0.048	0.660	0.040
33	181-02	564 m	*Lymnaea*	4	2	0.682	0.035	0.683	0.037
31	177-02B	552 m	*Helisoma*	10	0	0.714	0.046	0.689	0.040
31	177-02B	552 m	*Amnicola*	6	2	0.719	0.053	0.725	0.070
31	177-02D	552 m	*Amnicola*	7	2	0.706	0.044	0.694	0.032
30	179-02	552 m	*Helisoma*	6	2	0.694	0.034	0.617	0.027
30	179-02	552 m	*Vorticifex*	9	1	0.649	0.068	0.604	0.060
Owens ostracode OIS 2									
OV-1	202-02	20.7 ka	*Candona*	19	1	0.448	0.015	0.298	0.012
Panamint ostracode OIS 2									
15	02AJ-03	17 ka	*Candona*	7	1	0.533	0.020	0.545	0.039
Owens gastropods OIS 2 and younger									
OV-1	202-02	20.7 ka	*Helisoma*	8	1	0.642	0.058	0.444	0.041
OV-1	202-02	20.7 ka	*Vorticifex*	6	1	0.615	0.048	0.458	0.028
OV-2	201-2B	9.9 ka	*Helisoma*	10	0	0.654	0.036	0.383	0.016
OV-2	201-2B	9.9 ka	*Vorticifex*	10	0	0.635	0.024	0.384	0.012
OV-2	201-2B	9.9 ka	*Valvata*	10	0	0.638	0.030	0.364	0.017
Interlaboratory Comparative Standards (Wehmiller, 1984)									
3834	ILC-A	–	–	2	0	0.383	0.001	0.194	0.002
3835	ILC-B	–	–	2	0	0.695	0.001	0.428	0.001
3836	ILC-C	–	–	2	0	0.854	0.006	0.846	0.011

*Ages are conventional ^{14}C ages in thousands of years before present (ka).
†n = number of separate subsamples, each composed of a single shell, used to calculate the sample D/L mean ± 1σ.
§ex = number of additional subsamples excluded from the analyses because the D/L ratios fell beyond 2σ of the mean of the others.

ranging from 20 to 125 g, were dissolved in diluted nitric acid to extract Cl, and 1–3 mg of $Na^{35}Cl$ isotopically labeled ($^{35}Cl/^{37}Cl$ = 99%) carrier was added during sample dissolution. The supernatant was centrifuged, and excess $AgNO_3$ was added to precipitate, as AgCl, the natural Cl and cosmogenic ^{36}Cl released from the calcite and the ^{35}Cl carrier.

The resulting AgCl precipitate was purified of S (which interferes with the ^{36}Cl analysis as the ^{36}S isobar) using standard procedures (Zreda, 1994). The purified and dried AgCl was then sent to the PRIME Laboratory at Purdue University for accelerator mass spectrometry analysis of the $^{36}Cl/Cl$ ratio and the $^{35}Cl/Cl$ ratio (Elmore et al., 1979). The spreadsheet program CHLOE (CHLOrine-36 Exposure age) was used to calculate the $^{36}Cl/Cl$ ratio and Cl concentration of the samples based on the $^{36}Cl/Cl$ and $^{35}Cl/Cl$ analyses, sample mass, and mass of added ^{35}Cl carrier (Table 3) (Phillips and Plummer, 1996).

The CHLOE value herein is based on the cosmogenic nuclide production equations summarized by Gosse and Phillips (2001). The high-energy cosmic-ray flux is calculated based on standard exponential attenuation with mass depth, and the spallation production rate is proportional to that flux. The model then uses this flux distribution as the source term for the calculation of the epithermal and thermal neutron fluxes by means of the diffusion equations derived by Phillips et al. (2001). The spatial distributions of low-energy neutron fluxes are used to calculate the ^{36}Cl production by epithermal and thermal neutron absorption. Production parameters given in Phillips et al. (2001) and Stone et al. (1998) are used in the model.

CHLOE also computes production rates due to primary and secondary effects of the cosmic-ray muon flux, using approaches analogous to those already described. The spatial scaling (latitude and elevation) in CHLOE is based on Lal (1991). No corrections to the production rate due to secular variation of the geomagnetic field were employed. The production parameters in Phillips et al. (2001) were calibrated using samples from the approximate age, elevation, and latitude of the Panamint Valley samples. Correction for secular variation using this data set did not produce a better calibration (Lal, 1991). Improved spatial and temporal scaling methods have recently been published, but they would not be consistent with the Phillips et al. (2001) calibration, and we do not believe that employing them on top of that calibration would improve dating accuracy. The program also computes the concentration of nucleogenic ^{36}Cl (i.e., produced as a secondary result of radioactive decay or fission reactions within the minerals) in the sample and subtracts it from the measured total ^{36}Cl to obtain the cosmogenic ^{36}Cl concentration.

Bulk chemical analyses were performed by X-ray fluorescence (XRF) and prompt gamma emission spectrometry but were not used to compute ages because the tufas contained significant amounts of detrital silicates that were not dissolved during the nitric acid processing of the samples. The samples were assumed to consist of calcite with minor trace elements. Based on stoichiometry and on measurements of trace elements, ages for all of the tufas were computed using the following composition: CaO 56%, CO_2 44%, B 20 ppm, Gd 12 ppm, Sm 12 ppm, U 2 ppm, and Th 1 ppm. Cl concentration and ^{36}Cl concentration were determined for each sample based on the ^{35}Cl carrier isotope-dilution mass spectrometry analyses.

Calculated ^{36}Cl ages are given in Table 3. Apparent cosmogenic ages are affected by erosion; therefore, ages in Table 3 are given for three hypothesized erosion rates: 0, 1, and 3 mm/k.y. Based on field observations and general observations of bare-rock calcite erosion rates in arid environments, we believe that the actual erosion rates probably lie between 1 and 3 mm/k.y. Fortunately, the ages are relatively insensitive to erosion rate. Reported ^{36}Cl age uncertainties reflect only ^{36}Cl analytical uncertainty and are given as plus or minus one standard deviation. These quoted uncertainties are undoubtedly an underestimate of the actual uncertainties. Empirical evidence indicates that a more complete evaluation of age uncertainty, including factors such as error in chemical analyses and uncertainty in production parameters, yields total age uncertainties in the range of 10%–15% (Phillips et al., 2001).

Thermoluminescence (TL) and Infrared Stimulated Luminescence (IRSL)

Samples for luminescence dating were collected from silty marl or massive silty sand associated with tufas. Samples were obtained by scraping away ~10 cm of sediment and hammering a 6.35-cm-diameter opaque polyvinyl chloride tube horizontally into the outcrop wall. The sediment cylinder recovered was capped and wrapped with black plastic for transport. Additional sediment was collected from inside the core hole for moisture and dose rate determinations. Samples were double sealed in airtight bags to prevent loss of moisture.

Luminescence analyses were carried out in subdued orange-light conditions. Five centimeters of sediment was removed from each end of the sample pipes to prevent the possibility of contaminated sediments being dated. This sediment was added to the bulk sample for dose rate estimation. Luminescence measurements were made on the central section of the sediment cylinder, which was least likely to have been exposed to sunlight during sampling.

Samples were treated with 10% HCl and 30% H_2O_2 to remove carbonates and organic matter and then sieved to extract the fine silt (because this was considered the dominant grain size for many of the sampled deposits). Both TL and IRSL (the optically stimulated luminescence that uses infrared wavelength stimulation on K-feldspars) were performed on a polymineralic (no mineral separation) fine silt fraction (4–11 μm).

All measurements were made at 30 °C for 40 s after a preheat step to 125 °C for 48 h. The extracts from all samples were dated using the total-bleach multiple-aliquot additive-dose (MAAD) method (Singhvi et al., 1982; Lang, 1994; Richardson et al., 1997; Forman and Pierson, 2002). At least two attempts were made per IRSL sample to provide MAAD ages. Anomalous fading tests on the stability of the luminescence signal indicated little to no signal instability (recording ratios of 0.88–1.11). These values are a ratio of luminescence emission after storage of

TABLE 3. ^{36}Cl SAMPLE DATA AND CALCULATED AGES

Map site #	Sample	Latitude (°N)	Longitude (°W)	Elevation (m)	S_T (unitless)	Cl (ppm)	$^{36}Cl/10^{15}$ Cl (unitless)	^{36}Cl age, assumed erosion rate (ka) 0 mm/k.y.	1 mm/k.y.	3 mm/k.y.	Sample notes
15	PV02-01	35.99698	117.31106	532	0.99	23.4	4370 ± 140	45.3 ± 1.6	46.0 ± 1.6	47.6 ± 1.8	Near Water Canyon: tufa mound in embayment
13	PV02-02	35.99902	117.30466	515	1.00	40.4	2820 ± 100	50.6 ± 1.9	51.2 ± 2.0	52.9 ± 2.1	Near Water Canyon: horst block surface near #1
16	PV02-03	35.99763	117.32088	572	1.00	40.3	3360 ± 90	57.8 ± 1.6	58.7 ± 1.7	61.0 ± 1.9	On volcanic mound near Water Canyon
39	PV02-04	35.98337	117.32168	611	0.98	12.9	2890 ± 80	15.3 ± 0.4	15.2 ± 0.4	15.6 ± 0.4	High shoreline at R.S.U. Smith's Water Canyon locality
2	PV02-05	36.30893	117.41958	517	0.99	26.4	3010 ± 70	34.9 ± 0.9	35.3 ± 0.9	36.2 ± 0.9	Lower tufa locality at N end of Ash Hill
1	PV02-06	36.37816	117.40315	479	0.91	119	306 ± 13	16.2 ± 0.7	16.2 ± 0.7	16.2 ± 0.7	Lake Island hill, 3 m above playa
60	PV02-07	36.38386	117.40585	531	0.86	158	1230 ± 60	93.4 ± 4.8	92.3 ± 4.8	95.8 ± 5.5	Lake Island hill, 16 m above cave

Note: S_T is the topographic shielding scaling factor. The uncertainties are 1σ.

>30–60 d divided by the immediate measurement; a ratio of 1.0 indicates stable luminescence.

Most ionizing radiation in the sediment is from the decay of isotopes in the uranium and thorium decay chains and the radioactive potassium isotope 40. Bulk samples of at least 600 g were collected from the sample sites after the luminescence sample had been taken. In the laboratory, the bulk samples were counted on a high-resolution gamma-ray spectrometer for measurements of uranium, thorium, and potassium. The cosmic-ray dose rate was estimated for each sample as a function of depth, altitude, and geomagnetic latitude (Prescott and Hutton, 1994). Disequilibrium (between U and Th elemental concentrations) was discovered in one sample, and no attempt was made to generate any IRSL ages from that site.

The water content was assessed in the laboratory using sealed field samples (generally ~1% ± 0.5%) that were taken before the luminescence sample was collected. An arbitrary value of the sample's saturation moisture content throughout its depositional lifetime was assumed to be either 15% or 20%. Saturation values used were 15% for sandier sediment and 20% for siltier sediment. Ages were generated using a dose rate that assumed a 15%–20% water content, as this was a midpoint between the very dry field moisture and a fully saturated field moisture of 25%–45%. Alpha and beta contributions to the dose rate were corrected for grain-size attenuation (Aitken, 1985).

Field moisture and saturation moisture (potential of the sediment for holding a certain % of water during periods of moisture influx) were routinely measured. For the Panamint samples, the field moisture was between 1% and 3%, and the saturation moisture was between 25% and 45%, depending on how much of the sample was fine-grained (silts/clays). The errors on the dose rate change with increased water content were ~0.1% per every 5% water increase. These are reflected in the dose rate error. The full range (20% ± 20%) is already accounted for in the change of the absorbed dose (dose rate) that the sample sees (again assuming linear uptake), assuming the moisture content was sometimes 1%, but other times more like 25%.

OSTRACODES AND MAJOR DISSOLVED-ION COMPOSITION

Jones (1966) and Eugster and Jones (1979) discussed how the solute composition of natural waters changes with mineral precipitation, water-rock interactions, clay-mineral exchange, or redox reactions. Briefly, the solutes in dilute meteoric waters become increasingly concentrated by evaporation (lower effective moisture, climate effect) and (or) solute input from water-rock reactions (chemical hydrology, hydrology effect) until calcite saturation is reached. Then, with continued evaporation and (or) input from water-rock reactions, calcite (or aragonite) precipitates variously under equilibrium or nonequilibrium conditions, resulting in the eventual depletion or enrichment of either Ca or total carbonate alkalinity (alk) at the $CaCO_3$ chemical divide. Depletion or enrichment occurs because cations (Ca) and anions (HCO_3, CO_3) are lost from solution in equivalent proportions to form $CaCO_3$, and the original alk/Ca (in equivalents) ratio is rarely equal to one.

The relative gain or loss of Ca or alk from the water establishes the alk/Ca value, either high or low, and defines a triple-point boundary (Forester et al., 2005; http://www.kent.edu/nanode/) between three major solute types (Table 4): (1) those dilute waters that are dominated by Ca and alk or in which those solutes are common; (2) those in which alk is enriched relative to Ca, and (3) those in which Ca is enriched relative to alk. Type one must be freshwater and types two and three are commonly saline water. Ostracodes are sensitive to all three solute types (Forester, 1983, 1986, 1987, 1991; Forester et al., 2005; Smith, 1993).

Water Chemistry—Owens River System

In Panamint Valley and nearby basins, type 1 waters are common, especially at higher elevation, and they also represent basin-inflow waters (Table 4; see examples in Bradbury and Forester, 2002). Lakes along the Owens River system, e.g., Owens, Searles, and also low-elevation groundwater discharge, are typically type 2 water because they are the product of volcanic rock-water reactions and evaporative concentration (Table 4; Eugster and Jones, 1979; Bradbury and Forester, 2002). Alluvial and regional aquifer groundwaters in Death Valley are typically type 1 water, whereas some type 3 groundwaters in the south end of Death Valley rich in Ca are interpreted as hydrothermally derived and related to a midcrustal magma body (Li et al., 1997; Steinkampf and Werrell, 2001).

We lack major dissolved-ion chemistry for waters in the Panamint Valley. However, as is true throughout the region, springs along the basin margin having water derived from an alluvial aquifer likely are type 1 waters. Carranza (1965) reported TDS values from two spring/wetlands in Panamint Valley with values of 5880 mg/L and 175,000 mg/L as well as a high Cl content (2250 and 15,000 mg/L) and neutral pH (8.0 and 7.5, respectively). These waters, like the hydrothermal waters in Death Valley, must be type 3 waters, because type 2 waters are characterized by very high pH (>9.0), as well as being Ca-depleted and alk-enriched (Forester et al., 2005).

There are several ostracode species in core and outcrop sediment samples from the Panamint Valley that are important for the paleohydrological interpretations, including *Candona caudata, Limnocythere ceriotuberosa, L. sappaensis, L. staplini, Cyprideis beaconensis,* and *C. salebrosa* (Table 4; Forester et al., 2005). Summaries of general hydrochemical and physical environmental habitats for each species as well as interpretations in the context of Panamint Valley paleoenvironments are summarized in Table 4 and at http://www.kent.edu/nanode/.

PLEISTOCENE LAKES

The following description of Pleistocene lakes in Panamint Valley is divided into three sections. The first section concerns correlation and paleoenvironmental indicators of the older, high-

TABLE 4. OSTRACODES AND MAJOR DISSOLVED-ION COMPOSITION

Ostracode	Hydrochemistry	Preferred paleoenvironment	Interpretation
Candona caudata	Lives in type 1 waters and has an upper total dissolved solids (TDS) tolerance of about 1500 mg/L (www.kent.edu/nanode/).	Lives in a variety of environments including streams (e.g., upper Owens River), flowing springs, and lakes supported by streamflow.	Its occurrence in the Panamint Valley was likely most common during times when a relatively dilute lake supported by significant Owens River flow existed. Alternatively, it could also have lived in the flow from large permanent freshwater springs, which would have been most common during high effective moisture climates.
Limnocythere ceriotuberosa	Lives in water with solutes that define a field that is approximately centered on the solute evolutionary triple-point junction, with an extension into type 2 waters (Forester et al., 2005; www.kent.edu/nanode/).	Lives in lakes and wetlands that often receive a seasonal pulse of surface water or groundwater, followed by seasonal evaporation, resulting in higher TDS.	This species signifies Owens River inflow. Because it can live in waters with solutes that are less evolved, i.e., lower alk/Ca ratio, than *L. sappaensis* (see text; Forester et al., 2005), it could live in the Panamint Valley during an Owens-filling phase as well as during all but the final evaporative falling phase.
Limnocythere sappaensis	Lives in waters with a wide TDS range (600 to 100,000 mg/L). It is restricted to waters having evolved type 2 solutes with an alk/Ca ratio (equivalents) of more than 7 (Forester, 1983, 1986; www.kent.edu/nanode/).	Lives in permanent or ephemeral lakes and wetlands or springs, which have evolved type 2 solutes. It is often the only ostracode in alkalinity-enriched saline lakes, where its shells frequently form coquinas. This species can not survive in type 1 or 3 waters.	In the Panamint Valley, *L. sappaensis* indicates times when the basin contained Owens River water that sustained stillstand lake levels or more likely falling lake levels due to evaporative loss of water. Because *L. sappaensis* is limited to type 2 solutes, it likely would not live in the Panamint Valley during the filling phase unless Owens River flow was low and the solutes were evolved.
Limnocythere staplini	Lives in waters with a wide TDS range (400 to over 100,000 mg/L; Delorme, 1989). It is restricted to waters having evolved type 3 solutes with an alk/Ca ratio (equivalents) commonly below 1 (Forester, 1983, 1986; www.kent.edu/nanode/).	Typically lives in permanent or ephemeral lakes and wetlands. *L. staplini* is often the only ostracode in Ca-enriched saline lakes, where its shells frequently form coquinas. This species cannot survive in type 1 or 2 waters.	Its dominance in samples from the core, taken at a low elevation, implies there was no flow from the Owens River entering the Panamint Valley during its lifetime. Moreover, the source of water supporting the lake and or wetlands contained type 3 solutes. Such waters, like those in Death Valley, are commonly hydrothermal in origin (see, e.g., Eugster and Jones, 1979; Li et al., 1997, for discussion).
Cyprideis beaconensis and *C. salebrosa*	They live in waters with a wide TDS range common to estuaries as well as inland environments. These species are restricted to type 3 solutes, although in low-TDS settings, they are tolerant of less evolved solutes (Forester, 1991; www.kent.edu/nanode/).	*C. beaconensis* is common in Pacific Coast estuaries, while *C. salebrosa* is common in Atlantic and Gulf of Mexico estuaries. Estuarine ostracodes, unlike most continental species, can only survive in permanent water settings, so continental occurrences are typically in springs and spring-supported wetlands.	The presence of *C. beaconensis* in the Panamint Basin core sediments implies a permanent source of type 3 water (no Owens flow), likely derived from hydrothermal water in a deep aquifer (see, e.g., Li et al., 1997). The presence of *Cyprideis* spp. in shoreline sediments with solute type 1 and 2 ostracodes represents a mixed-species assemblage, implying basin-margin deep groundwater discharge mixed with lake water. Mixing type 2 and 3 waters will commonly precipitate tufas. The existence of *C. salebrosa* this far west implies different migratory bird routes in the past than today.

elevation Gale strandlines (Smith, 1976), which lie between 550 and 600 m elevation. These strandlines are constrained to be older than ca. 50–70 ka and younger than the 620 ka Lava Creek B Tuff (Vogel et al., 2002). The second section describes new paleontological information about the fossil-bearing section of the archived core collected by Smith and Pratt (1957). The core provides insight into the sources of water for the OIS 2 lake and for the older, shallow lake and wetland deposits that probably range in age from about OIS 3 to OIS 5. The third section describes evidence for the shoreline elevation and source of lacustrine water during OIS 2, based primarily on surface exposures, a 4 m auger sample, and new ^{14}C ages (Tables 1A and 1B).

Highstand (Gale) Strandlines

The Gale strandlines have been previously mapped between ~600 and 560 m elevation in the basin (Smith, 1976). We collected samples from five areas: Nadeau Road, upper Water Canyon wash, and lower Water Canyon wash in the Ballarat basin; and Big Four Mine road and Panamint Springs in the Lake Hill basin (Fig. 1). Lacustrine and wetland gastropods including *Carinifex* sp., *Amnicola* sp., and *Valvata* sp. are abundant in nearshore deposits above 550 m elevation, but they are far rarer and generally sparse at lower elevations. They were not found below 415 m elevation in surficial deposits exposed in the basin. Fine-grained, friable, silty marl was collected that contained ostracode assemblages that were used for paleoenvironmental determinations. The Nadeau Road locality was also sampled for IRSL/TL analysis.

Nadeau Road

The Nadeau Road site lies west of the Ash Hill fault on the flanks of Bendire Canyon between ~580 and 597 m elevation. Hanna (1963) described a diverse aquatic gastropod fauna at 561 m elevation from this site and also noted that the assemblage was nearly identical to that collected from high shorelines in the Searles Lake Basin. The assemblage was identified as *Limnaea* (*Polyrhytis*) *kingii* (Meek), *Stagnicloa kingii* (Meek), *Lymnaea kingii* (Meek), *Radix ampla,* and *Galba utahensi*s. The stratigraphy of the site includes a coarse, cross-bedded cobble beach deposit that overlies a whitish, silty, fossiliferous, diatomaceous marl (Figs. 3A–3C) (Smith, 1976). Algal tufa mounds overlie beach deposits and are interbedded with the beach gravels; large colonial mounds also underlie the whitish marl.

Eight samples were collected from an ~1.5 m section of diatomaceous marl for ostracode identification. Two samples were collected for IRSL/TL analysis, one from the overlying silt and one from near the base of the section (site 40, Fig. 3B, Table 5; and AJ-4 and AJ-5, Table 6). The fine-grained sediment contains a diverse ostracode assemblage (Table 5) including rare *Limnocythere ceriotuberosa,* which is indicative of cold, fresh to saline, high alk/Ca solute–dominated waters, suggesting an Owens River source. The presence of *L. ceriotuberosa* implies a filling or through-flowing lake, or a terminal lake that is not losing much water to evaporation. *Cyprideis salebrosa* is an estuarine species common to the Gulf of Mexico along the Atlantic coast as well as inland saline springs east of the Rocky Mountains. The assemblage of *Cyprideis salebrosa, Cypridopsis vidua, Limnocythere* n sp., *Limnocythere ceriotuberosa,* and *Limnocythere itasca* indicates a low alk/Ca solute–dominated water, suggesting a deep groundwater source discharging on the margin of a lake. The site is proximal to the Ash Hill fault zone, which may have produced localized groundwater discharge.

The silt that overlies the diatomaceous marl and underlies the cross-bedded cobble beach conglomerate gave IRSL and TL ages, respectively, of 13.7 and 21.3 ka near the top of the section (sample AJ-4, Fig. 3B, Table 6). IRSL and TL ages of 51.3 and 64.6 ka were obtained near the base of the diatomaceous marl section (AJ-5, Fig. 3B, Table 6). Fitzpatrick and Bischoff (1993) obtained a ca. 24 ± 1.0 ka U-series age on tufa from this site. The anomalously young U-series and IRSL/TL ages suggest that the deposit was open to groundwater or spring discharge, and they are not considered to be indicative of the age of deposition (Fitzpatrick and Bischoff, 1993).

Upper Water Canyon

The upper Water Canyon site (Smith, 1976) lies in the western Ballarat basin between ~610 and 585 m elevation where beach and nearshore deposits overlie Paleozoic bedrock south of the active wash (Fig. 1). This is one of the best-known highstand beach deposits in the Panamint Valley. The site lies on the opposite side of the valley from the well-preserved shorelines mapped by Smith (1976) near Ballarat (Fig. 4A).

The upper Water Canyon location includes a well-developed abrasion surface at ~610 m elevation overlain by large (meter-scale) colonial-type algal tufa and thick aquatic gastropod coquinas cemented by tufa and pebble-cobble beach deposits (Figs. 4B–4D; Smith, 1976). Gastropod coquinas dominated by *Helisoma newberri* and *Stagnicola* sp. are also interbedded with ~1–10-m-thick diatomaceous silt and marl (Fig. 4D). Gastropods were analyzed for AAR from site 38 at this locality (Tables 1 and 4). Two U-series ages of 66 and 54 ka on tufa are considered minimum ages (Fitzpatrick and Bischoff, 1993).

Lower Water Canyon

The lower Water Canyon sample sites lie in the western Ballarat basin between ~551 and 563 m elevation north of Water Canyon wash (Fig. 1). Lacustrine and wetlands deposits are preserved on the west side of a horst block that lies east of the Ash Hill fault zone. Cobble beach lag clasts, tufa, and silty marl overlie an eroded Tertiary volcanic bedrock surface at ~551–560 m elevation.

At site 30 (Figs. 1, 5A, 5B), charophytic tufa rests directly on bedrock, and lag clasts of a cobble beach deposit are present at ~555 m elevation. Downslope a few meters, tufa locally overlies gastropod-bearing silt, which overlies silty whitish marl (Fig. 5B, with hand auger in sample hole). Gastropods collected from 555 m elevation at ~25 cm depth were dated at 32,550 ± 270 ^{14}C yr B.P. (Jayko et al., 2001), but we consider this age to be a limiting minimum, as secondary calcareous cement or tufa was present on the shells. No evidence was found elsewhere in the basin for an OIS 2 strandline at this elevation.

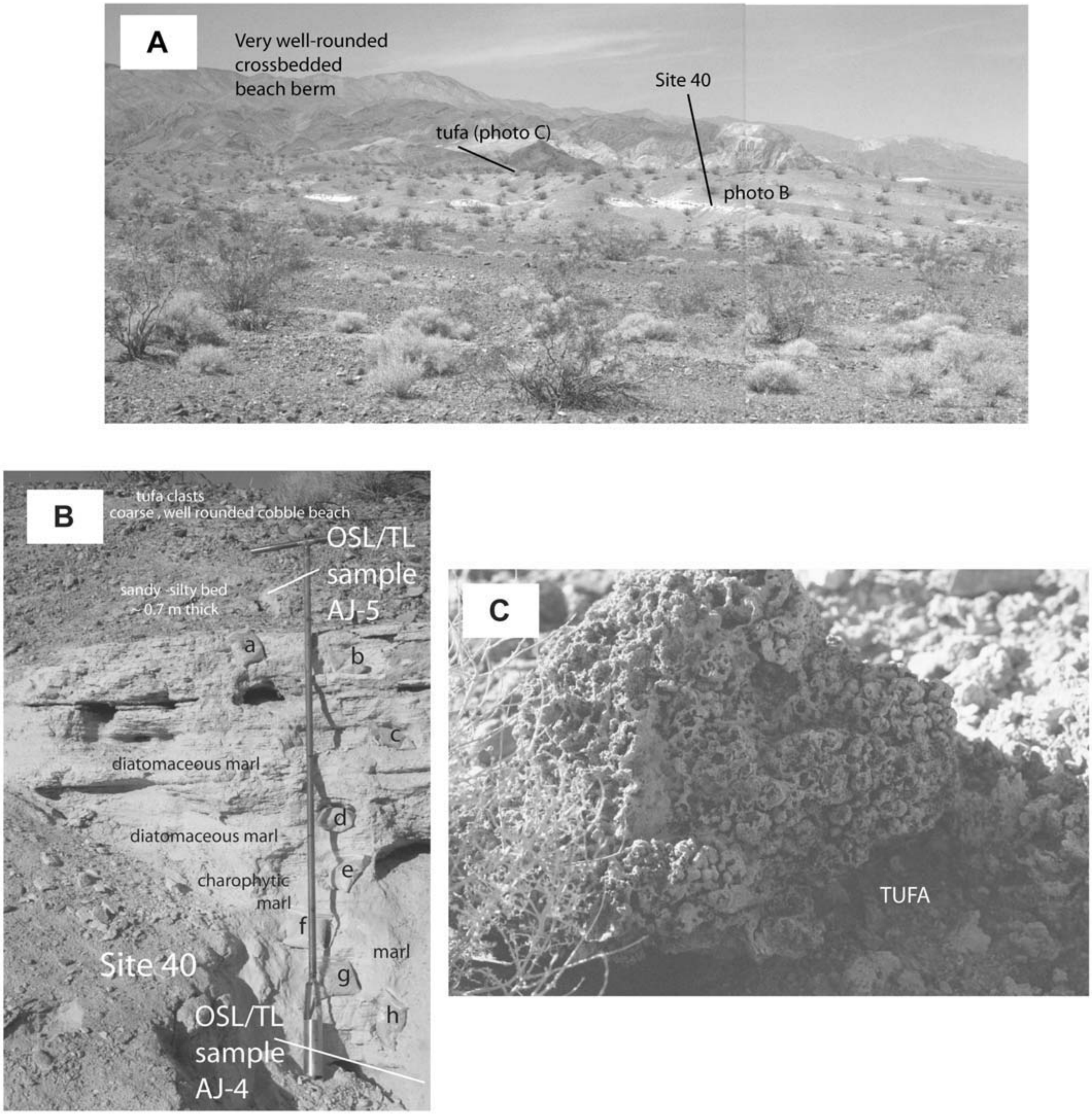

Figure 3. Photographs of site 40, located at ~570 m elevation on the Nadeau Road. (A) Location of lacustrine deposits. (B) Diatomaceous marl and overlying silt where samples were collected for IRSL-OSL (infrared stimulated luminescence–optically stimulated luminescence)/thermoluminescence (TL) and ostracode paleoecology. (C) Large mound of lacey orbicular tufa that overlies well-rounded, well-sorted beach cobbles.

At site 31 (Figs. 1, 5A, 5C), marl is exposed in the floor of the wash to ~20 cm above the base of the wash. The marl is overlain by angular-subangular alluvium derived from Paleozoic bedrock to the west, which is in turn overlain by colluvium derived from the Tertiary volcanic rock exposed on the horst block to the east (Fig. 5C). An ~40-cm-deep auger sample was taken at this locality. Gastropods are abundant in the silty marl from the top of the marl in the wash exposure to ~20 cm depth. The marl is underlain by compacted gastropod-barren mud. Gastropods were auger-sampled at 20 cm depth for AAR analysis (Table 2, field ID 177–02).

Site 33 lies at ~564 m elevation where silty whitish marl and local 10–20-cm-thick gastropod-bearing coquina beds are

TABLE 5. OSTRACODES FROM SURFICIAL DEPOSITS AND DH-1 CORE

Sample number	Map sites Figure 3	Shoreline or sample elevation (m)	*Limnocythere sappaensis*	*Potamocypris* sp.	*Potamocypris unicaudata*	*Sarscypridopsis aculeata*	*Cavernocypris* sp.	*Darwinula* sp.	*Cyprideis* sp.	*Cyprideis salebrosa*	*Cyprideis beaconensis*	*Cypridopsis vidua*	*Limnocythere* n sp.	*Limnocythere ceriotuberosa*	*Limnocythere staplini*	*Limnocythere itasca*	*Heterocypris incongruens*	*Heterocypris* sp.	Groundwater *candonid*	*Candona* sp.	*Candona patzcuaro*	*Cypridopsis vidua*	*Candona rawsoni* group	*Candona caudata*	*Cytherissa lacustris*	Other	*Elphidium* sp. (foraminifera)	Gastropod shell	*Chara* spp.	Root tubes	^{14}C (ka)	Amino acid
01 MNE-1b	3	351																														
01 MSE-2a	8	415	x																												Table 5	
02 AJ-3	17	415	x											x										x	c						Table 5	
auger 397-407	A	468	x																												Table 5	
01 MNE-3b	18	488															x														Table 5	
01 MNE-3c	18	488																								Fish bone?					Table 5	
02 MPSE-1	19	512	x											x						x											Table 5	
		0 0												GALE STRAND -LINES																		
01 PS-2b	50	555																										x				
GPS 177-02A	31	552											x							x			x		x			x				X
GPS 180-02B	32	555							x							x							x	x				x		x		
GPS 181-02B	33	564												x								x	x	x				x		x		X
GPS 183-02B	34	582											x			x						x						x	x			
GPS 193-02	51	597							x	x			x			x	x					x		x				x	x			X
GPS 187-02B	36	604								x				x								x						x	x			X
GPS 189-02	38	604																										x		x		X
01 SR-2	39	604																							x	Dia-toms						
02 AJ-4	40	597								x		x	x	x		x												x	x Marl			
		Depth (m)																														
DH-1 core	**DH-1**																															
(interval in ft)	**DH-1** **DH-1**																															
DH-1, 9–12'	**DH-1**	–3.2									x				x																	
DH-1, 12–67.7'	**DH-1**	–14								bar-ren																						
DH-1, 67.8–70.5	**DH-1**	–21													x																	

(*continued*)

TABLE 5. OSTRACODES FROM SURFICIAL DEPOSITS AND DH-1 CORE (*continued*)

Sample number	Map sites Figure 3	Shoreline or sample elevation (m)	*Limnocythere sappaensis*	*Potamocypris* sp.	*Potamocypris unicaudata*	*Sarscypridopsis aculeata*	*Cavernocypris* sp.	*Darwinula* sp.	*Cyprideis* sp.	*Cyprideis salebrosa*	*Cyprideis beaconensis*	*Cypridopsis vidua*	*Limnocythere* n sp.	*Limnocythere ceriotuberosa*	*Limnocythere staplini*	*Limnocythere itasca*	*Heterocypris incongruens*	*Heterocypris* sp.	Groundwater *candonid*	*Candona* sp.	*Candona patzcuaro*	*Cypridopsis vidua*	*Candona rawsoni* group	*Candona caudata*	*Cytherissa lacustris*	Other	*Elphidium* sp. (foraminifera)	Gastropod shell	*Chara* spp.	Root tubes	^{14}C (ka)	Amino acid
DH-1,70.8–73.5	**DH-1**	–22	x												x																	
DH-1, 73.8–76.9	**DH-1**	–23	x				x	x							x			x														
DH-1, 79.9–82.9	**DH-1**	–24	x				x							x	x			x	x													
DH-1, 79.9–82.9	**DH-1**	–25	x											x	x			x														
DH-1, 82.9–87.5	**DH-1**	–26	x					x						x	x			x														
DH-1, 87.5–90.5	**DH-1**	–27	x				x								x			x														
DH-1, 90.5–93.5	**DH-1**	–28	x		x		x							x	x			x														
DH-1, 97'	**DH-1**	–29.6										x		x	x											Volcanic glass						
DH-1, 98'	**DH-1**	–29.9							x						x																	
DH-1, 99'	**DH-1**	–30.2										x																		x	24,880 ± 160	
DH-1, 100'	**DH-1**	–30.5																														
DH-1, 100.9'	**DH-1**	–30.7													x																	
DH-1, 101'	**DH-1**	–30.8																														
DH-1, 112'	**DH-1**	–34.14									x				x					x												X
DH-1, 114'	**DH-1**	–34.75																														
DH-1, 115'	**DH-1**	–35													x, coquina																	
DH-1 122.4–123.4	**DH-1**	–37.5									x				x					x									x			
DH-1 125.4–128.4	**DH-1**	–38.8			x						x				x					x									x	x		
DH-1 128.4–131.4	**DH-1**	–39.5									x				x					x									x			
DH-1 131.4–134.4	**DH-1**	–40.4									x				x					x	x						x		x		40,720 ± 670	X
DH-1 134.4–137.4	**DH-1**	–41.45				x					x				x					x							x	x	x		Abundant forams	

(*continued*)

TABLE 5. OSTRACODES FROM SURFICIAL DEPOSITS AND DH-1 CORE (*continued*)

Sample number	Map sites Figure 3	Shoreline or sample elevation (m)	*Limnocythere sappaensis*	*Potamocypris* sp.	*Potamocypris unicaudata*	*Sarscypridopsis aculeata*	*Cavernocypris* sp.	*Darwinula* sp.	*Cyprideis* sp.	*Cyprideis salebrosa*	*Cyprideis beaconensis*	*Cypridopsis vidua*	*Limnocythere* n sp.	*Limnocythere ceriotuberosa*	*Limnocythere staplini*	*Limnocythere itasca*	*Heterocypris incongruens*	*Heterocypris* sp.	Groundwater *candonid*	*Candona* sp.	*Candona patzcuaro*	*Cypridopsis vidua*	*Candona rawsoni* group	*Candona caudata*	*Cytherissa lacustris*	Other	*Elphidium* sp. (foraminifera)	Gastropod shell	*Chara* spp.	Root tubes	^{14}C (ka)	Amino acid
DH-1 137.4–140.4	**DH-1**	–42									x				x														x			
DH-1 143.4–147.4	**DH-1**	–43.3									x				x																	
DH-1 147.4–150.4	**DH-1**	–45.42									x				x					x									x			
DH-1 150.4–153.3	**DH-1**	–46.33			x						x				x					x									x			
DH-1 153.3–162.2	**DH-1**	–48.2									x				x					x								x	x			
DH-1 162.3–172.2	**DH-1**	–50.9																														
DH-1 172–175	**DH-1**	–53																														
			MISS-ING																													
DH-1 175–192	**DH-1**	–55.6				x									x											*Ruppia* sp.			x			
DH-1 191–194	**DH-1**	*–58.7*			*x*						*x*	*x*			*x*		*x*			*x*	*x*					*Ruppia* sp.		*x*	*x*			
DH-1 194–197	**DH-1**	–59.6			x						x				x					x						*Ruppia* sp.		x	x			
DH-1 197–200	**DH-1**	–60.5			x	x					x				x		x									*Ruppia* sp.			x			
DH-1 205–208	**DH-1**	–62.9				x					x	x			x																	
DH-1 208–218	**DH-1**	*–64.9*																														
			MISS-ING																													
DH-1 255–259	**DH-1**	*–78.3*									*x*				*x*																	
DH-1 270–278	**DH-1**	*–83.5*									*x*																					
DH-1 278–280	**DH-1**	*–85*																														
Pan-2 ~ 280'	**DH-1**								x						x																	

(*continued*)

TABLE 5. OSTRACODES FROM SURFICIAL DEPOSITS AND DH-1 CORE (*continued*)

Sample number	Map sites Figure 3	Shoreline or sample elevation (m)	*Limnocythere sappaensis*	*Potamocypris* sp.	*Potamocypris unicaudata*	*Sarscypridopsis aculeata*	*Cavernocypris* sp.	*Darwinula* sp.	*Cyprideis* sp.	*Cyprideis salebrosa*	*Cyprideis beaconensis*	*Cypridopsis vidua*	*Limnocythere* n sp.	*Limnocythere ceriotuberosa*	*Limnocythere staplini*	*Limnocythere itasca*	*Heterocypris incongruens*	*Heterocypris* sp.	Groundwater *candonid*	*Candona* sp.	*Candona patzcuaro*	*Cypridopsis vidua*	*Candona rawsoni* group	*Candona caudata*	*Cytherissa lacustris*	Other	*Elphidium* sp. (foraminifera)	Gastropod shell	*Chara* spp.	Root tubes	^{14}C (ka)	Amino acid
DH-1 284–287	**DH-1**										x				x					x												
DH-1 287–290	**DH-1**	–88		x							x				x																	
DH-1 290–292	**DH-1**	–89									x				x																	
DH-1 295–298	**DH-1**	–90													r																	
DH-1 298–301	**DH-1**	–91													r																	
DH-1 308.5–311.5	**DH-1**	–95																		x												
DH-1 314.5–317.5	**DH-1**	–96									r															Charo-phyte						
DH-1 317.5–321.8	**DH-1**	–97									r			x	x																	
DH-1 321.8–324.8	**DH-1**	–98									r																					
DH-1 324.8–327.5	**DH-1**	~100 m									r																					

TABLE 6. GAMMA SPECTROMETRY ANALYSES ON ELEMENTAL DATA FOR DOSE RATES, EQUIVALENT DOSE DATA, AND RESULTING IRSL AND TL AGES

Sample number (site number)	Location and elevation (m)	% Water content*	K (%)	Th (ppm)	U (ppm)	Cosmic dose† additions (Gy/k.y.)	Total dose rate (Gy/k.y.)§	Equivalent dose (Gy)	Age (ka)	Method
AJ-1	Panamint Spings	1 ± 0.5	1.33 ± 0.02	11.8 ± 0.36	9.01 ± 0.21 #	0.21 ± 0.02	6.29 ± 0.12	357 ± 12.7	56.7 ± 4.58	IRSL
(50)	548–555							415 ± 16.6	66.0 ± 5.84	IRSL
	delta foreset									
	deposit						6.62 ± 0.13	315 ± 17.5	47.5 ± 5.67	TL
	stratigraphically									
	above AJ-2							445 ± 36.0	67.3 ± 11.2	TL
AJ-2	Panamint Springs	2 ± 0.5	2.35 ± 0.03	23.1 ± 0.56	5.72 ± 0.39	0.19 ± 0.02	7.11 ± 0.15	292 ± 1.84	41.0 ± 1.80	IRSL
(50)	548–555							317 ± 5.00	44.6 ± 2.34	IRSL
	delta foreset						7.48 ± 0.16	258 ± 4.13	34.5 ± 1.82	TL
	deposit							376 ± 41.0	50.3 ± 11.1	TL
AJ-3	Lower Shepherd	1 ± 0.5	1.14 ± 0.02	7.22 ± 0.29	11.9 ± 0.15 #	0.19 ± 0.02	6.74 ± 0.11	288 ± 2.02	>42.7 ± 1.48	IRSL
(17)	Canyon Fan								disequilibrium	
	415–418									
AJ-4	Nadeau Road	3 ± 0.5	2.58 ± 0.02	9.81 ± 0.28	4.71 ± 0.13	0.19 ± 0.02	5.63 ± 0.13	77.2 ± 0.69	13.7 ± 0.51	IRSL
(40)	597							80.4 ± 1.13	14.3 ± 0.62	IRSL
							5.93 ± 0.10	113 ± 9.15	19.1 ± 3.17	TL
								126 ± 2.18	21.3 ± 1.08	TL
							4.00 ± 0.07**	61.1 ± 0.67**	15.2 ± 0.38**	OSL
AJ-5	Nadeau Road	2 ± 0.5	2.59 ± 0.03	11.2 ± 0.49	3.45 ± 0.25	0.18 ± 0.02	5.26 ± 0.16	270 ± 3.40	51.3 ± 3.24	IRSL
(40)	594						5.54 ± 0.16	358 ± 0.14	64.6 ± 6.21	TL

Notes: IRSL—infrared stimulated luminescence; TL—thermoluminescence; OSL—optically stimulated luminescence. Ages are based on dose rates of 15% moisture content through time for AJ-4, AJ-5 (sandy sediment), and 20% moisture for AJ-1, AJ-2, AJ-3 (silty sediment). In all samples, the silt fraction was run (4–11 μm size), except for the quartz blue light age; for AJ-4, the fine sand fraction (90–125 μm size) was used.

*Field moisture, ages based on 15%–20% (sand-silt) moisture content through time as an average between field and saturation moisture values.

#Analyses show disequilibrium in U/Th ratios, and resulting ages were not used in results or discussion.

†Cosmic doses and attenuation with depth were calculated using the methods of Prescott and Hutton (1994).

§Dose rate and age for fine-grained polymineral silt (IRSL or TL, with TL dose rate always larger). Exponential regression used on age, errors to one sigma.

**Dose rate and age for 90–125 um quartz sand (blue-light OSL). Exponential regression used on 24 (of 28; 4 failed runs) aliquots for age, errors to one sigma.

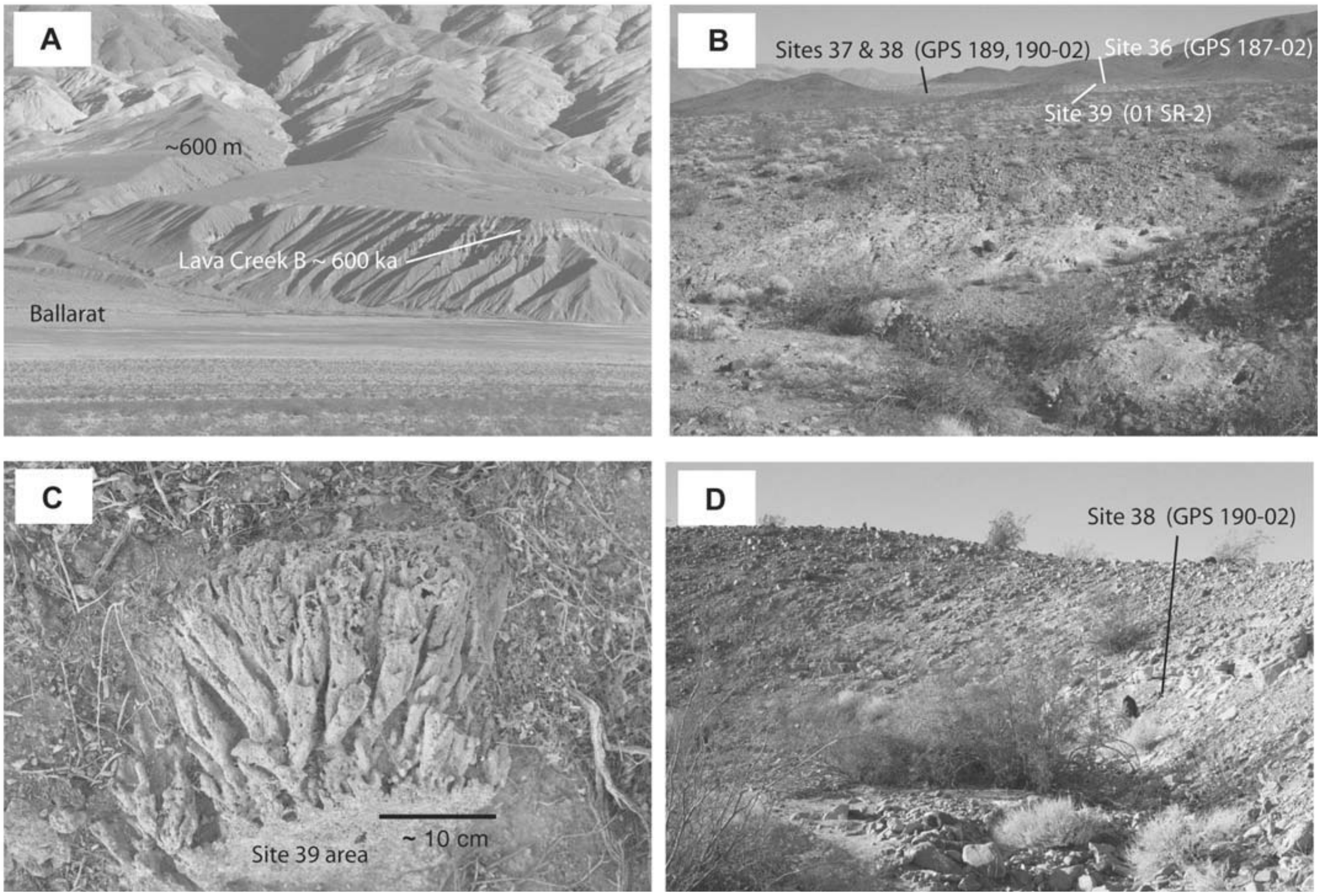

Figure 4. Photographs of sites constraining age of Gale strandline. (A) Pleistocene alluvial gravels near Ballarat with overlying abrasion surface and Pleistocene shorelines. Zircons from tephra at the base of the section are ca. 900 ka (Vogel et al., 2002), and two higher tuff beds are stratigraphically correlative with the Bishop Tuff (760 ka) and Lava Creek B ash (ca. 620 ka), constraining the shoreline age and discharge to Death Valley to be younger than 600 ka. (B) Location of sample sites south of Water Canyon at ~600 m elevation. (C) Colonial or coralline-type algal tufa. (D) Location of sample collected for amino acid racemization (AAR) analysis at site 38. Backpack for scale near bottom of leader.

exposed in a wash cut (Figs. 5D and 5F). The marl is overlain by ~3–4 m of weathered alluvium with distinct rubified clay films present. The north-facing wash cut was excavated and sampled for gastropods and ostracodes (Table 5). A bed of well-rounded beach cobbles overlies siltstone and marl up-wash from this site at ~580–585 m elevation (Fig. 5E, site 34).

Big Four Mine Road

The Big Four Mine site (Davis, 1970; Smith, 1976) lies between ~560 and 597 m elevation on the east side of the Lake Hill basin south of the Big Four Mine road. The deposits are preserved on a horst block that lies west of the Panamint fault zone. The top of the horst block is flattened by a wave-cut abrasion surface, and the west side of the horst exhibits a wave-cut notch overlain by well-bedded, thinly laminated, fine-grained sediment and marl deposits. Gastropods and ostracodes were collected for AAR analysis from this site (Table 2). Davis (1970) reported a finite, ca. 52 ka ^{14}C age from this site during archaeological investigations of the Lake Hill area.

Panamint Springs Delta Foresets

Delta foreset deposits were recognized by Hall and MacKevett (1962) and Smith (1976) in small bluffs a few hundred meters northeast of Panamint Springs between ~548 and 555 m elevation. A thinly bedded, gastropod-rich horizon and recessional beach deposit overlie the delta foreset beds. Although this locality contains some thinly bedded marls with 10–30-cm-thick gastropod coquinas, the preservation of both ostracodes and gastropods from this locality is extremely poor. The gastropods are altered and thus too friable to collect. Two samples for IRSL/TL analysis were collected from sandy silt that underlies the gastropod-bearing horizon. Sample AJ-1 gave TL ages of 47.5 ± 5.7 to 67.3 ± 11.2 ka; however, the down-section and stratigraphically lower sample AJ-2 gave TL ages of 34.5 ± 1.87 to 50.3 ± 11.1

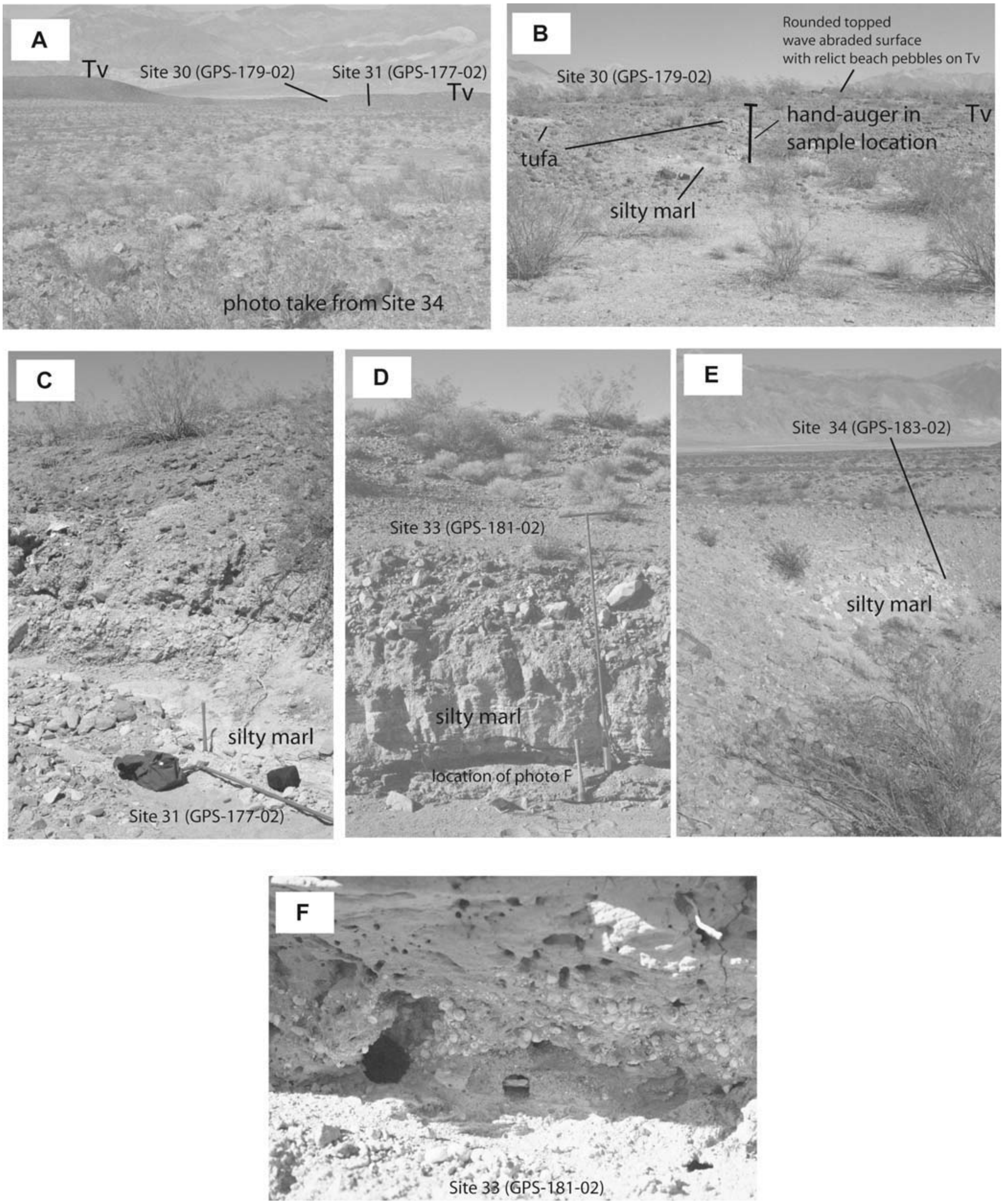

Figure 5. Photographs of sites constraining age of Gale strandline. (A) View looking east showing location of sites 30 and 31 at ~550 m elevation where samples were taken for amino acid racemization (AAR) on gastropods and ostracodes. The sites are inset on eroded Tertiary volcanic rock (Tv). Hill behind the sites is upthrown Tertiary volcanic rock that lies on the east side of a strand of the southern part of the Ash Hill fault zone. (B) Depositional features at site 30, including tufa overlying bedrock and marl; auger is located in sample hole. (C) Marl exposed in wash at site 31 with shovel handle at sample site. (D) Marl with gastropod coquina exposed at site 33 in wash at ~555 m elevation. (E) White silty marl overlain by very well-rounded beach cobbles. (F) Close-up of gastropod coquina from site 33.

(Table 6). These ages are considered minima because paleoecological results from core DH-1 described in the next section preclude a large deep lake during this time interval. The elevation of this location exceeds the divide that separates the basins by ~35 m; thus, deltaic deposits at this elevation indicate a single large lake in Panamint Valley.

Summary of Highstand Paleoenvironmental Indicators

The ostracode assemblage (Table 5) from the deposits at 550–600 m elevation indicates mixing of water discharged from a regional groundwater aquifer near active faults with the cold fresh lake (cf. Forester et al., 2005). Groundwater discharge may be fault-controlled along the Ash Hill fault at the Nadeau Road locality and the Panamint fault zone at the Lake Hill Mine locality. The second ostracode assemblage contains species, including *Cyprideis beaconensis,* that require low alk/Ca, type 3 solutes, which may indicate an origin similar to the $CaCl_2$ waters that discharge from springs at the southern end of Death Valley today (Li et al., 1997). *Cyprideis salebrosa* is common in this modern assemblage today and is also found living inland in springs east of the Rocky Mountains where it is associated with bird flyways from the Gulf of Mexico. We speculate that its presence may imply that bird flyways during the time of deposition were west-northwestward rather than north-south, likely due to continental glaciers covering the northern land area.

Correlation of the Gale Highstand Deposits

Three sites were selected for AAR analysis (Fig. 1; Table 2): upper Water Canyon, lower Water Canyon, and the Big Four Mine Road. Gastropods of the genera *Helisoma* (*Carinifex*), *Vorticifex, Amnicola, Lymnaea,* and *Valvata,* and ostracodes of the genus *Candona* were analyzed. Two or more genera, each comprising a separate sample, were analyzed from most stratigraphic horizons. *Helisoma* (*Carinifex*) *newberri* was the most common gastropod genus. The rate of racemization in this taxon was compared with several others in stratigraphic horizons where they co-occurred with other species (Table 2). The results show that both Asp and Glu racemize at the same rate in *Helisoma,* as with all the gastropod genera analyzed in this study except for *Amnicola,* which exhibits higher ratios. The data also show the expected difference between the much higher rates of racemization in gastropods compared with ostracodes (e.g., Laabs and Kaufman, 2003) from the same stratigraphic horizon (Fig. 6).

The extent of AAR can be used to estimate numerical ages where the rate of racemization is calibrated based on independent age control for a particular region and a particular taxon. Ages for the gastropods from Panamint Valley can be estimated roughly by comparing D/L ratios with other snails of known ages, combined with reasonable assumptions about temperature history. For this analysis, we focused on the Glu data, which seem to provide the most reliable chronometer for gastropods with D/L > 0.5 (e.g., Laabs and Kaufman, 2003). We rely on the calibration curve derived for dated shells from in and around the Grand Canyon (Kaufman et al., 2002).

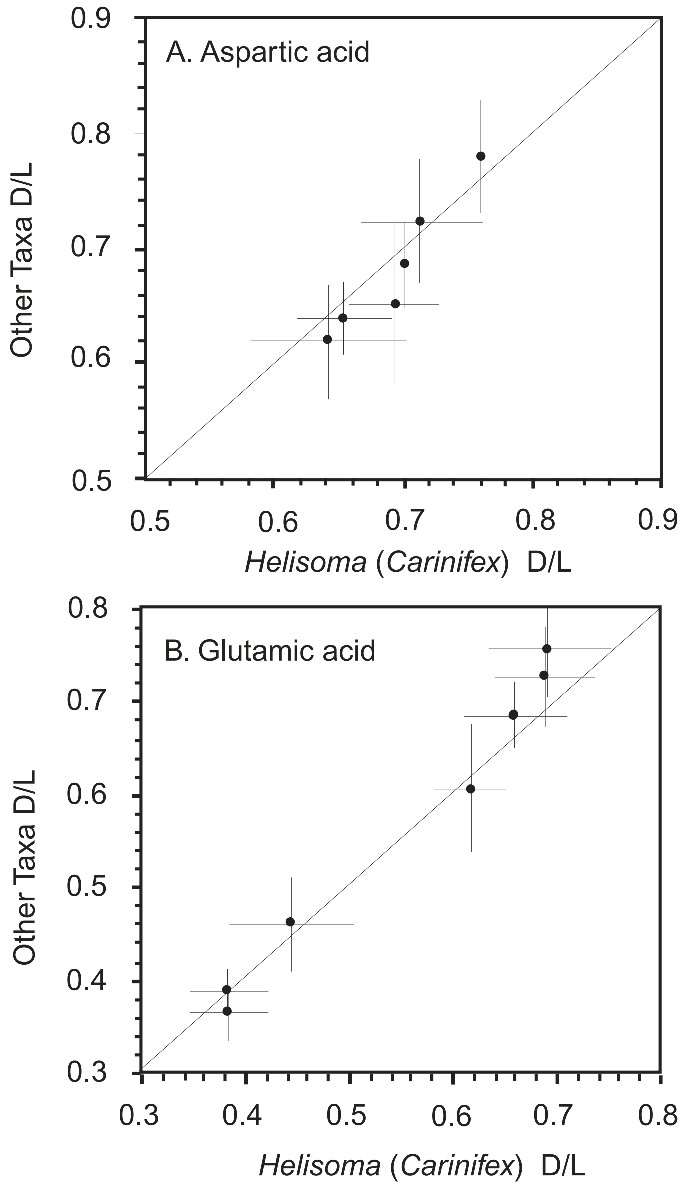

Figure 6. Comparison of the extent of racemization (D/L) in coeval samples of *Carinifex* and other gastropod taxa (data in Table 6) from the same stratigraphic unit for (A) aspartic acid and (B) glutamic acid. Error bars are ±1σ of multiple subsamples (intershell variation). Lines show one-to-one relations.

Application of the D/L values from Panamint Valley to this calibration yields an average age of ca. 210 ka for the 550 and 610 m shorelines. Because the D/L values in gastropods from these two shorelines overlap, so do their ages. This estimate is probably a maximum age because temperatures in Panamint Valley are higher by at least several degrees, and therefore the long-term rate of racemization is probably higher in Panamint Valley compared with the sites used to derive the Grand Canyon calibration curve (Kaufman et al., 2002). Higher late Quaternary temperatures are inferred from a comparison between present mean annual temperatures, which are ~18 °C for Panamint Valley and

16 °C for the Grand Canyon samples. Qualitatively, on the basis of the difference in temperature, the maximum ages estimated for the Panamint Valley shorelines are probably several tens of thousands of years too old. An age approximately in the range of OIS 6 is permissible based on this analysis.

The ^{36}Cl results (Table 3) give disparate ages, some of which are younger than independent geological and geochronological data. We have identified four possible origins for apparent bias: (1) chemical erosion of the tufa surfaces, (2) coverage of the tufa by lacustrine or alluvial deposits that have subsequently been eroded away, (3) fractionation of Cl isotopes during dissolution of the samples in nitric acid, and (4) loss of ^{36}Cl during subaerial recrystallization or diagenesis of the tufa.

Hypothesis 1 is discounted because we calculated apparent age as a function of erosion rate, and the variation in age was not nearly large enough to explain any potential discrepancies. With regard to hypothesis 2, review of field notes indicated that all of the samples except PV02-04 were from situations where prior coverage by lacustrine or alluvial sediment (or other surficial cover such as dune sand or loess) was highly unlikely. PV02-04 could potentially have been covered by lacustrine sediment, and we attribute its highly anomalously young age most probably to this cause. We evaluated hypothesis 3 by comparing the results of closed-vessel dissolutions with the open-vessel method that was used for the Panamint samples and found no systematic bias. We therefore suggest that the ^{36}Cl ages for at least some of the tufa samples may be biased by solution and recrystallization of the tufa (hypothesis 4).

We have previously conducted methodological tests using Last Glacial Maximum–age tufa from Lake Lahontan and Searles Lake, and the ^{36}Cl ages here are in excellent agreement with the independent dates (F.M. Phillips, 2006, personal commun.). However, those samples were much younger than the probable age of most Panamint Valley tufas and were also quite dense and nonporous. In contrast, many tufa heads in Panamint Valley have a sponge-like morphology. Petrographic examination of these specimens did not yield conclusive evidence either for or against recrystallization (S. Roof, 2005, personal commun.). In summary, anomalously young ^{36}Cl ages due to subaerial recrystallization would appear to be a distinct possibility for at least some Panamint tufas, but more research is needed to establish the extent of this problem.

Sample PV02-04 at 611 m yielded an apparent ^{36}Cl age of ca. 16 ka, but we believe that this was due to prior coverage by lacustrine sediment. Likewise, IRSL/TL analysis on siltstone and marl from the same locality gave ca. 14 and ca. 20 ka ages, respectively, at 597 m elevation (AJ-4, Table 6), probably indicating resetting associated with groundwater discharge or eolian silt accumulation during the late Pleistocene. At lower elevations in the southern basin where ^{14}C ages of 14,000–22,000 yr B.P. (~506–518 m) have been determined on tufa, ^{36}Cl analyses gave ages ranging from ca. 48 to ca. 61 ka (PV02-1, PV02-2, PV02-3; Table 3) for samples that ranged in elevation from 515 to 572 m. These results are probably best interpreted as indicating that lake stands above ~518 m are older than OIS 3, and perhaps much older.

A few hundred meters southeast of Ballarat (Fig. 4A), the highstand shorelines at ~560–590 m elevation are inset into alluvial-fan deposits that contain the 620 ka Lava Creek B tuff. It occurs near the top of the 80-m-thick alluvial section (Vogel et al., 2002) and underlies the Gale strandline deposits, which include tufa and beach cobbles (Smith, 1976). Thus, the Gale strandlines must be younger than 620 ka.

Panamint DH-1 Core

Three >100-m-long cores, DH-1&1a, DH-2, and DH-3, were drilled in Panamint Valley during the 1950s (Smith and Pratt, 1957) and subsequently archived in Menlo Park, California, at USGS. DH-1&1a and DH-3 were located in the Ballarat basin, and DH-2 was located in the Lake Hill basin. DH-3 was located close to the basin depocenter, reached ~325 m depth, and contained thick salt beds; however, it was sparsely fossiliferous to unfossiliferous. DH-3 core samples have previously been dated using meteoric ^{36}Cl and U-series analyses (Jannik et al., 1991; Fitzpatrick et al., 1993) that have loosely constrained the ages of subsurface deposits (Fig. 2). A third core drilled in the Lake Hill playa that reached Paleozoic rock at ~125 m depth (Smith and Pratt, 1957) was not reinvestigated in this study. Part of the DH-1&1a core contains a fossiliferous section between ~3 and 100 m depth where microfauna had been previously noted but not identified.

We sampled the DH-1&1a core for two ^{14}C ages from near the top of the microfossil-bearing section (Tables 1B and 5), ostracode paleoenvironmental indicators throughout the fossil-bearing part of the core (Table 5), and two AAR analyses (Fig. 2; Tables 2 and 5). Fifty samples were collected from ~100 m of core for faunal analysis (Fig. 2), and thirty samples between ~30–85 m depths were based on lithologic descriptions from Smith and Pratt (1957). Plant material from 30.5 m depth yielded an age of 24,880 ± 160 ^{14}C yr B.P. (Tables 1B and 5). One hand-picked monospecific sample consisting of *Cyprideis beaconensis* from 39.5 m depth was dated by AMS at 40,710 ± 670 ^{14}C yr B.P. (Tables 1B and 5). The age is considered a minimum for this depth in the section.

Samples selected for AAR analysis at 40.4 m and 59.3 m depth were from at least 40,710 ± 670 ^{14}C yr B.P. in the DH-1 core. The D/L values in these two ostracode samples are lower than those obtained from two OIS 2 localities in Owens Valley (Fig. 1). These results suggest that the AAR rate is significantly slower for the deeply buried core samples compared to samples from surficial outcrops in Owens Valley, where higher ambient temperatures may have accelerated the AAR rate. Therefore, we could not use the AAR results from the core to help constrain the age of surficial shoreline deposits in Panamint Valley.

Cyprideis beaconensis and *Limnocythere staplini,* indicative of type 3 water (Table 4), and abundant brine shrimp pellets occur between 37.5 and 60.5 m depth in DH-1 (Table 5). This assemblage, indicative of a saline groundwater-supported brine, probably occupied a marsh, wetlands, and/or shallow lacustrine environment. The estuarine foraminifera *Elphidium* sp. occurs at 40–41.8 m depth and is locally abundant, indicating it was living in the wetlands. Its occurrence is also indicative of a low alk/Ca ratio, and a water chemistry similar to the ocean. Seeds identified as *Ruppia* sp. by Laura Strickland, U.S. Geological Survey (Denver), suggest water depths of less than 4 m and a generally silty-sandy substrate rather than mud or clay, consistent with a shallow water body. The presence of *Limnocythere staplini* in this interval indicates TDS concentration <100 g/L. The section between 63 and 78 m depth is barren and (or) the core was not recovered, and between 78 and ~99 m depth, it is again dominated by ostracodes that require a shallow, low alk/Ca groundwater source (Tables 3 and 4; Forester et al., 2005).

Summary of DH-1 Core Results

Between 34 and 63 m depth, DH-1 contains *Cyprideis beaconensis* (Tables 4 and 5), which is indicative of low-alkalinity and high-Ca groundwater discharge from a regional, and likely thermal, groundwater source (cf. Li et al., 1997). Floral and faunal remains between 34 and ~100 m depth indicate a shallow lake or wetlands and the absence of Owens River–type water (type 2, Table 4). The dominance of *C. beaconensis* and *L. staplini* in the 35 and 100 m depth range also indicates that shallow saline lake and wetlands conditions persisted during this interval.

Age constraints from two ^{14}C ages near the top of the core (Fig. 2) suggest maximum sedimentation rates of ~0.8–1.2 mm/yr. Sedimentation rates from the Death Valley core mainly range between ~0.8 and 1.0 mm/yr at depths between 8 and 182 m (Lowenstein et al., 1999; Forester et al., 2005). This sedimentation rate, and somewhat lower rates, are also typical of late Pleistocene sections in adjacent basins, including Searles and Owens Valleys (Smith et al., 1983; Smith and Bischoff, 1997; Bischoff and Cummins, 2001; Jayko, 2005). An assumed sedimentation rate between 0.7 and 1.0 mm/yr for the 100-m-thick section of shallow lake and wetlands sediments in the Panamint Valley core suggests a span of time of ~70–100 k.y., and thus the section below the lower ^{14}C date probably includes the entire OIS 4 interval.

The wetlands and shallow lake were supported by a low alk/Ca, type 3 groundwater indicative of a deep, probably thermally heated, regional aquifer that was discharging along the major active faults in the basin (Tables 3 and 4). Likewise, the halite-dominated evaporite-mineral assemblage in the core is consistent with a local rather than Owens River source (Jannik et al., 1991). There is no indication from the core samples for the high alk/Ca Owens River inflow or a large lake in Panamint Valley during OIS 4, so these results negate the likelihood of overflow into the basin. However, the presence of large saline wetlands or a shallow lake in the center of Ballarat basin indicates significantly wetter conditions than today.

OIS 2 Lake

Radiocarbon ages from shoreline charophytic and stromatolitic algal tufas combined with ostracode assemblages from (1) a shallow auger core from the Lake Hill basin, (2) archived DH-1 core from Ballarat basin, and (3) nearshore deposits located on the western slopes of Ballarat basin suggest that a large, ~180–200-m-deep lake occupied Panamint Valley during OIS 2. The ostracodes indicate that the valley was receiving water from the Owens River system and likely serving as a terminal lake where water loss was largely to evaporation rather than outflow during this time.

Lake Hill Area

Tufa ringing Lake Hill at ~475 m elevation yielded ages of 13,000 ± 1000 ^{14}C yr B.P. (Davis, 1970) and 11,800 ± 70 ^{14}C yr B.P. (Jayko et al., 2001) (Fig. 1; Table 1A). Tufa from this elevation also gave a 16,200 ± 700 yr ^{36}Cl age (Figs. 1 and 3). Another tufa site at ~500 m elevation near the north end of Ash Hill, within the Lake Hill basin, gave ages of 14,950 ± 80 ^{14}C yr B.P. and 34,900 ± 900 yr ^{36}Cl.

A 4-m-deep hole was augered near a trench locality at Lake Hill where previous archaeological investigations reported ages of 10,520 ± 140 and 10,020 ± 120 ^{14}C yr B.P. on peat-bearing sediment at ~2.15 m depth (Davis, 1970; Hubbs et al., 1965). The auger hole was sampled at ~15 cm intervals. The stratigraphy of the 4-m-deep hole consists of a basal meter of fine-grained mud and clay, organic-rich silt, and ~2 m of overlying silt, sand, and grit deposits (Fig. 7; Table 1B). A *Limnocythere sappaensis* coquina is present between the 3–4 m interval, which lies at ~467 m elevation. This assemblage indicates an alkaline-saline lake supported by inflow of Owens River water likely into a terminal lake undergoing evaporative concentration (i.e., with high salinity). The lacustrine mud is overlain by ~1 m of organic-rich sediment that contains molluskan and ostracode fauna, indicating a freshwater wetland and spring discharge environment (Fig. 7).

A 16,735 ± 50 ^{14}C yr B.P. age on *Limnocythere sappaensis* shells from the base of the auger sample at ~4 m depth indicates that a lake with Owens River–type water chemistry was still present in the upper basin, and that Searles Basin was still likely overflowing into Panamint Valley or had been overflowing in the recent past. Aquatic gastropods from the base of the peat or "black mat" at 3.08–3.16 m depth gave an age of 12,575 ± 40 ^{14}C yr B.P. for the drying of the lake and the development of shallow wetlands supported by groundwater discharge. The ostracode and mollusk species assemblages indicate the presence of a perennial marsh or shallow lakeshore environment during the latest Pleistocene at ~468 m elevation.

OIS 2 Record in DH-1 Core

Limnocythere sappaensis is found in the DH-1 core between 21.3 and 27.5 m depth in the Ballarat basin (Tables 4 and 5). *Limnocythere sappaensis* appears to be reworked in the upper part of the section where it occurs between 21.3 and 25.3 m depth, and it appears in situ between 25.3 and 27.5 m depth. An age of 24,880 ± 160 ^{14}C yr B.P. was obtained from carbonaceous material at 30.2 m depth, indicating an OIS 2 age for this part of the core. This age-depth relation gives an ~1.2 mm/yr

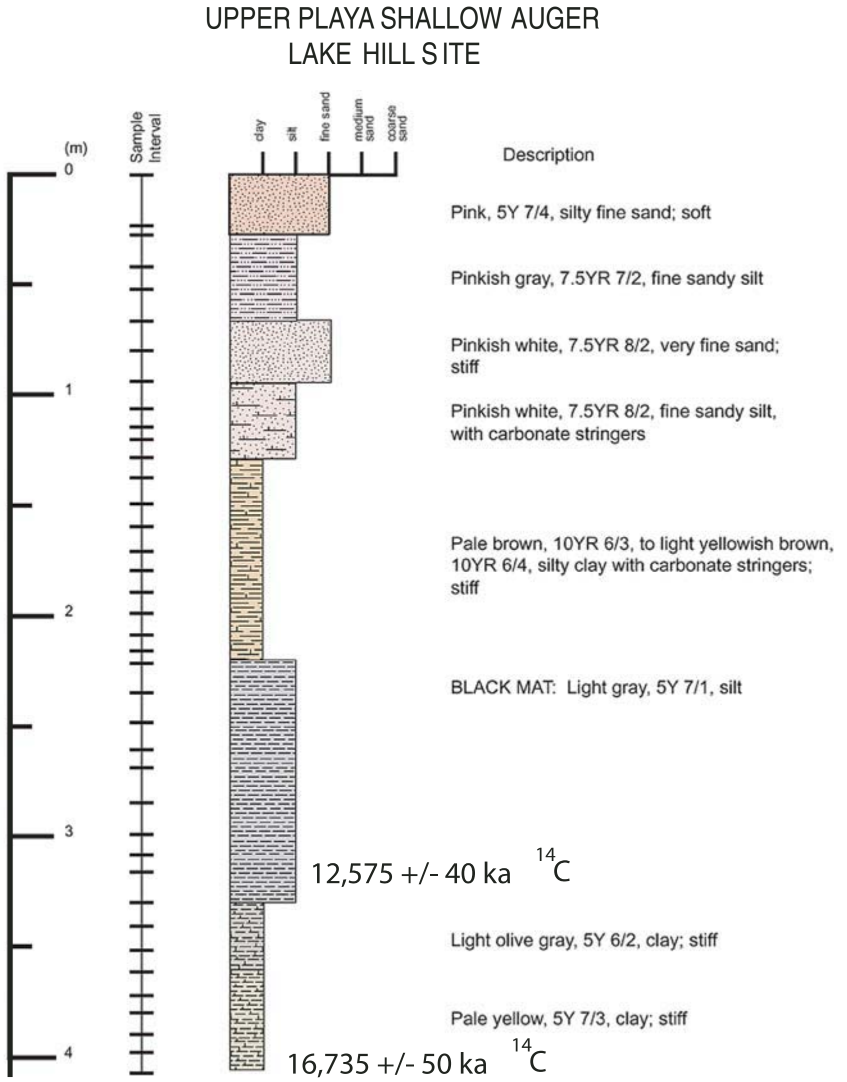

Figure 7. 4 m auger site A from Lake Hill basin, southern tip of Lake Hill, showing stratigraphic profile, paleoenvironmental interpretation, and ^{14}C ages.

0 - 216 cm PLAYA AND INTERMITTENT SPRINGS-WETLANDS

Dominantly clastic sediment, clast size (grit-clay) variable, few fossils represented by occasional ostracodes, snail shells and one sample with bone. The section has variable amounts of root, trace carbonate, some carbonate that resembles efflorescent crust, and some gypsum. Woody material and seeds are also present. One sample contains part of a conchostracan (?) carapace (clam shrimp).

216 - 308 cm WETLANDS

Well preserved and abundant ostracodes and snails. The upper sample has abundant carbonate (the capping carbonate phase of wetlands). Ostracode species are indicative of spring and seep discharge and not indicative of lacustrine, extensive wetlands or flow environments. The oldest sample with only spring and wetland ostracodes and mollusks occurs within the 299-308 cm interval.

308 - 330 cm MAINLY WETLANDS

Mix of wetland fauna and rare *Limnocythere sappaensis* (indicates alkaline saline lake). From 316-330 cm *Limnocythere sappaensis* in poor shape with reworked other ostracodes.

330 - 407 cm ALKALINE-SALINE LAKE

Limnocythere sappaensis abundant, good preservation, no other ostracodes. Indicates deposition in an alkaline saline lake suggesting one contiguous lake in the basin (thus, the two Panamint basin lakes are likely merged) or hydrological exchange. *Limnocythere sappaensis* coquinas persist to the bottom sample, so lake did not attain a chemistry dilute enough to have *Limnocythere ceriotuberosa.*

sedimentation rate. An estimation of the age for the *L. sappaensis*–bearing part of the core using the 1.2 mm/yr rate suggests ca. 24–21 ka (Table 5).

Nearshore Deposits and Erosion Features

Charophyte and other algal tufa associated with well-rounded beach gravels from several localities between 512 and 360 m have yielded ~14,000–28,000 ^{14}C yr B.P. ages (Fig. 1; Table 1A; site descriptions). Three tufa sites with late-glacial ^{14}C ages are described here: (1) southern Ash Hill fault horst blocks north of lower Water Canyon, (2) lower Shepherd fan, and (3) Surprise Canyon fan. In addition, the erosion features around the south-facing side of the divide between the Ballarat and Lake Hill basins are noted.

Southern Ash Hill fault horst blocks, lower Water Canyon. Massive reefal tufa overlain by tufa-cemented pebble beach gravel lies at ~512 m elevation inset on Tertiary andesitic volcanic rock (Fig. 8A; Fig. 1, site 15). Both bedded-pea-gravel and cobble beach deposits form a discontinuous shoreline around the Tertiary bedrock knoll at site 15 and nearby. The beach cobbles are generally monolithologic, very well rounded, and derive directly from the underlying Tertiary volcanic bedrock, and thus they have not been transported by fluvial or other processes to the location (Fig. 8B). The material upslope from the beach gravels contrasts markedly in its angular clasts and abrupt upslope change in clast morphology (Fig. 9C).

Due east of site 15, across a narrow half-graben, lies a wave-cut abrasion surface at ~506 m elevation that is overlain by charophytic tufa on the south-facing side of the surface and by relict well-rounded beach clasts (Fig. 9D). The flat abrasion surface is developed on top of the horst block that lies within the southern part of the Ash Hill fault zone.

Four ^{14}C ages from both the massive 1- to 2-m-thick reefal tufa and thinner 5- to 15-cm-thick charophytic tufa deposits on the

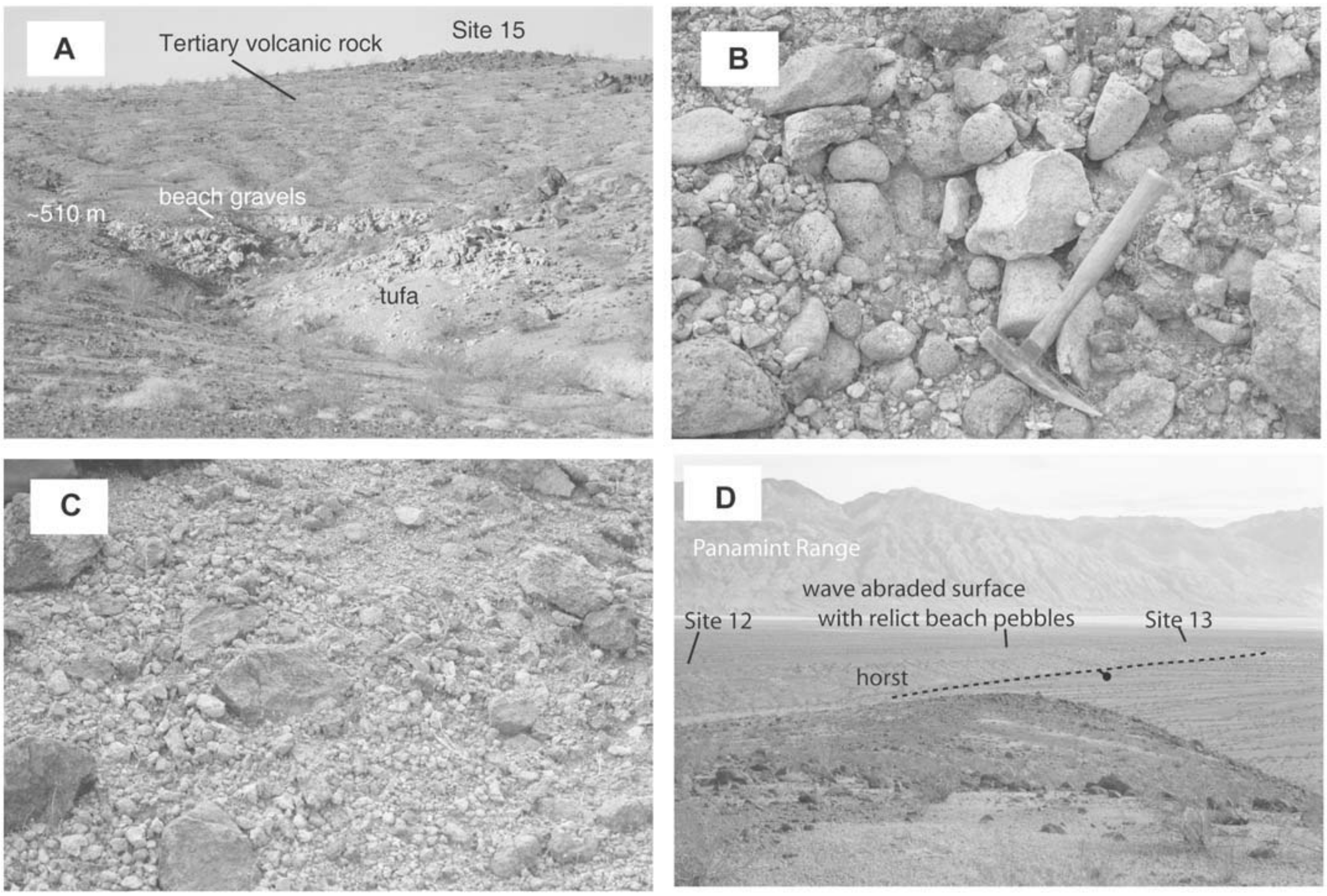

Figure 8. Photographs constraining age and height of oxygen isotope stage (OIS) 2 strandlines. (A) Reefal tufa at site 15, 510 m elevation with ^{14}C age of 22,600 ± 130 yr B.P. (B) Well-rounded cobbles from beach at 510 m elevation near site 15. The clasts are monolithologic and derived exclusively from the underlying Tertiary volcanic bedrock. (C) Angular, monolithologic colluvium derived from Tertiary volcanic bedrock upslope from the relict cobble beach deposit. (D) Smooth flat wave-cut abrasion surface at sites 12 and 13, developed on horst block within the southern part of Ash Hill fault zone east of site 15.

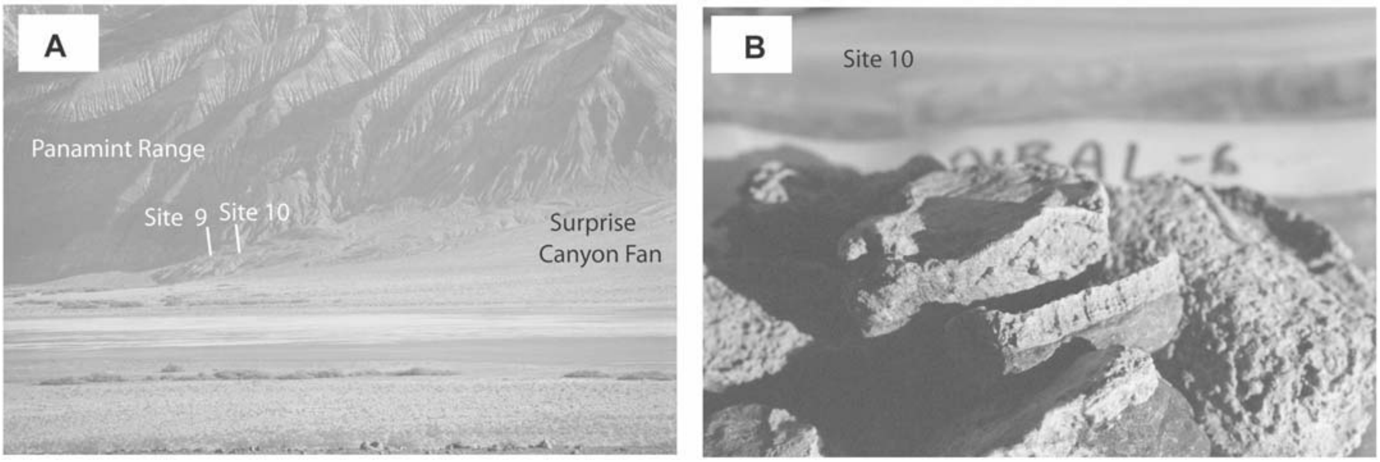

Figure 9. Photographs of oxygen isotope stage (OIS) 2 deposits at the north end of the Surprise Canyon fan north of Ballarat. (A) Location of sites 9 and 10. (B) Close-up of mini-atoll–like stromatolitic algal tufa on well-rounded beach cobbles found at the sites.

abrasion surface range from 18,000 to 28,000 yr B.P. (Table 1B; Fig. 1). However, ^{36}Cl results from two of the same exposures are 45,300 ± 1600 and 50,600 ± 1900 yr B.P. (Table 3). Horst blocks within the Ash Hill fault zone that are present downslope from 512 m elevation also have beveled or abraded, smooth and flat-topped, pavement-covered, charophytic tufa-bearing surfaces (cf. Figs. 1 and 9D).

The Basin divide. The divide between the Ballarat and Lake Hill basins presently lies at ~521 m elevation; however, active tectonism may have increased the elevation of this feature since deposition. A large cobble beach berm straddles much of the lowest part of the divide, but this wave-controlled feature is interpreted as a relict from recession of the older Gale highstand. The south-facing side of the basin divide has a continuous trimline or wave-cut edge at ~512 m elevation. An abrasion or wave-cut surface is present between ~496 and 512 m and is overlain by an eolian reworked sandy deposit. A thick deposit of carbonate forms a knickpoint at ~512 m elevation in the wash draining the Argus Range to the west. The carbonate ledge is interpreted as having formed in a groundwater-discharge area adjacent to the shore.

Surprise Canyon fan. Accumulations of well-rounded, cobble beach deposits and wave-cut notches are preserved on small, fault-controlled horst blocks that offset the north slope of the Surprise Canyon fan (Fig. 9A). The beach deposits occur between 400 and 430 m elevation. Rare, well-rounded cobble clasts with mini-atoll stromatolitic reefs (Fig. 9B) were dated from these deposits at sites 9 and 10 using ^{14}C. Stromatolitic carbonate rinds from the clasts gave ages of 14,150 ± 80 and 22,570 ± 110 ^{14}C yr B.P. at ~415 m elevation (Table 1; Fig. 1).

Lower Shepherd Canyon fan. The lower part of the Shepherd Canyon fan (Fig. 1, site 8) is incised by a wash where an exposure at ~384 m elevation contains a thin bed of silty marl that overlies whitish brecciated tufa (Figs. 10B–10D). The silty, whitish marl is overlain by ~1.15 m of alluvial gravel capped by an incipient, strongly oxidized pavement surface (Fig. 11A). Soil development in the overlying alluvial deposit is incipient, and only disparate, locally developed thin rinds of carbonate coatings occur on the underside of some clasts. This grayish-weathering alluvium contrasts with the redder, more weathered alluvium overlying similar silty marls above 552 m elevation.

The marl contains a monospecific assemblage of *Limnocythere sappaensis* indicative of type 2, high alk/Ca lacustrine water in a terminal lake sourced by the Owens River system (Forester, 2001; Forester et al., 2005). About 50–60 m upslope in the same wash (Fig. 1, site 17), the marl contains a mixed lacustrine and wetlands ostracode assemblage (Table 5, site 17). Large clasts of whitish brecciated tufa (Fig. 10C), with large bladed crystalline structures resembling thinolite (?), underlies the marl (Fig. 10D). This form of tufa resembles coarse crystalline tufa that encrusts tree stumps at Mono Lake and contrasts markedly in color and morphology with the other generally pinkish-cream– colored charophytic and algal tufa deposits found at higher elevation. We infer that this brecciated tufa deposit may represent a collapsed tufa tower. The tufa gave an age of 17,130 ± 100 ^{14}C yr B.P. (Table 1).

Summary—OIS 2 Lake

Charophyte and other algal tufas associated with beach deposits and abrasion surfaces give ^{14}C ages of ca. 24–14 ka (OIS 2) from elevations ranging between 518 and 384 m in the Ballarat basin (Table 1; Fig. 1). If the ^{14}C ages are reliable, then the OIS 2 highstand reached ~518 m at ca. 24,000 ^{14}C yr B.P. and possibly a second time around 18,000–16,000 ^{14}C yr B.P. (Fig. 11; Table 1). This strandline elevation and the equivalent lacustrine sediment in the core suggest that an ~180–200-m-deep lake occupied the Ballarat basin of Panamint Valley during OIS 2. However, it is important to note that collocated ^{14}C and ^{36}Cl samples collected at both the northern Ash Hill and lower Water Canyon sites gave discrepant results, with ^{14}C ages of ca. 15–28 ka and ^{36}Cl ages of ca. 35–50 ka. This discrepancy indicates potential problems. For example, the tufas that have given Last Glacial Maximum (LGM)

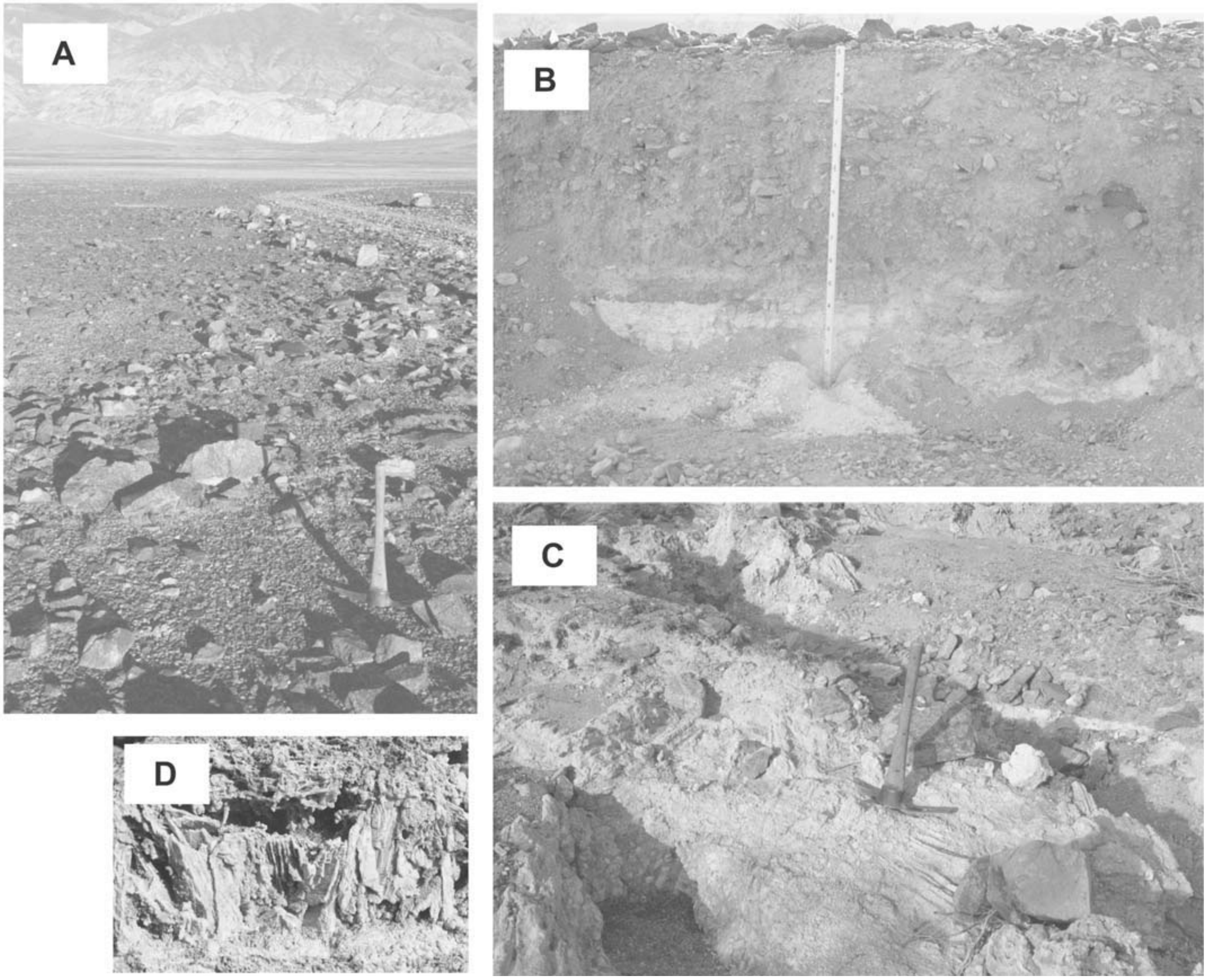

Figure 10. Photographs of oxygen isotope stage (OIS) 2 deposits in Shepherd fan. (A) Varnished pavement surface overlying ~1.0–1.5 m of alluvial gravel at site 8. (B) Whitish marl with lacustrine and wetland ostracodes underlying ~1.1 m of poorly consolidated alluvial gravel with weakly developed stage 1 carbonate at site 8. (C) Brecciated spring-mound–type tufa underlying marl of photo A. (D) Close-up of bladed tufa at site 8.

ages may be contaminated by young carbon, the LGM shoreline may have reoccupied an older shoreline at ~500 m, or there may be problems in the ^{36}Cl model ages as suggested by results from the higher-elevation strandlines.

Limnocythere sappaensis was found in association with *L. ceriotuberosa* and *Candona* sp. in surficial deposits (Table 5, sites 17 and 19), which are indicative of nearshore environments, at ~415 and 512 m elevation in the Ballarat basin. The presence of these three species may reflect deposition when the OIS 2 lake was shifting from a filling to a falling lake. *Limnocythere sappaensis* in the nearshore deposits, the shallow auger sample, and the DH-1 core together suggest that Owens River water was flowing into the basin between ca. 24,000 and 15,550 ^{14}C yr B.P. Ostracode species indicative of type 3 water, which characterizes the deep aquifer discharge in Panamint Valley, do not survive in the Owens River–type water chemistry (Forester, 1983, 1999; Forester et al., 2005) and were not found in these deposits.

Results of augering combined with a tufa "bathtub" ring confirm the presence of a shallow lake in the Lake Hill basin during the latest Pleistocene, consistent with the finding of Smith (1976). The ostracode *Limnocythere sappaensis* indicates that high alk/Ca, type 2 water dominated the lacustrine environment, indicating an Owens River source (cf. Forester, 2001). Ostracode assemblages indicate type 2, Owens River–system chemistry in both Lake Hill and Ballarat basins, suggesting hydrologic connectivity, either via surface or groundwater flow, between the two basins across a divide that presently lies at ~521 m. The auger results indicate the termination of the lake in Lake Hill basin by

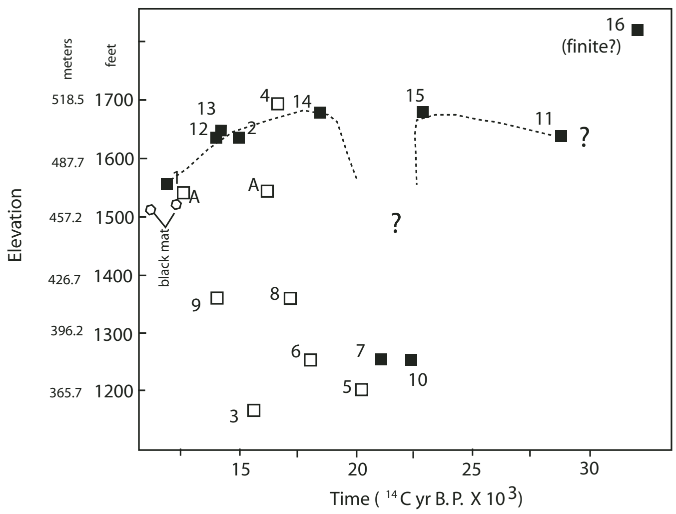

Figure 11. Plot showing time versus elevation with ^{14}C dated deposits and tufas. Results may indicate that the oxygen isotope stage (OIS) 2 highstand lowered briefly around 19–21 ^{14}C ka; however, this is highly speculative, and the reliability of the tufa ages has not yet been established. The OIS 2 lake was desiccated by around 12.5 ^{14}C ka, and extensive springs dried up by around 10–10.5 ^{14}C ka, as indicated by ^{14}C ages of the black mats. Black squares—beach and nearshore material described in Table 1A, open squares—lacustrine, open hexagons—black mat deposit at Lake Hill.

the end of the Pleistocene, but before 12,575 ± 40 ^{14}C yr B.P. (Jayko et al., 2002).

The saline lake in Lake Hill basin receded before ~12,575 ± 40 ^{14}C yr B.P. (Fig. 7; Table 1B) and was replaced by a groundwater-supported wetlands based on ostracode assemblages and stratigraphic succession. Peat found by Davis's (1970) archaeological investigation is underlain by mud and silt containing *Assiminea* n. sp., *Tryonia porrecta* (*protea*), and *Gyraulus circumstriatus* between 2.04 and 2.15 m below the surface of the playa near Lake Hill (Taylor, 1986; *T. protea* revised to *T. porrecta* in Hershler, 1999).

The Lake Hill site is the only known occurrence of coexisting *Assiminea* n. sp. and *Tryonia porrecta* (*protea*) (Taylor, 1986). This spring and wetlands gastropod assemblage has not yet been found in the older highstand wetlands and shoreline deposits during this or previous investigations. Modern populations of *Assiminea* are known in the Death Valley–Ash Meadows area (Taylor, 1986). *Tryonia porrecta* (*protea*), to the exclusion of other *Tryonia* species, is known from the lower Owens River and its former watercourse (Taylor, 1986), and it occurs in association with other *Tryonia* species throughout the Great Basin and lower Colorado River Basin (Hershler, 1999; Hershler et al., 1999).

Gyraulus circumstriatus has a modern widespread range in the west but is presently restricted to environments ~1500 m higher than Lake Hill at this latitude (Taylor, 1986). This gastropod suggests colder ambient temperatures around 13,000 yr ago, probably equivalent to today's mean annual temperature at around 3000 m elevation. The terrestrial gastropods *Vertigo berryi, Succinea* sp., and the common bivalve *Pisidium casertanum* are also present (Taylor, 1986) and indicate groundwater-supported wetlands (Hershler, 1999). The wetlands persisted between ca. 12,575 and 10,500–10,000 ^{14}C yr B.P., when the setting became a dry playa.

DISCUSSION

Results from Panamint Valley appear to be consistent with core records from Owens Valley and Death Valley, which both contained lakes during OIS 2 and OIS 6. There is no evidence for a cold, deep lake or Owens River–type water in Death Valley during OIS 4 (Lowenstein et al., 1999; Bradbury and Forester, 2002; Forester et al., 2005). Open basin conditions and discharge toward Searles Lake persisted during OIS 4 in Owens Valley (Carter, 1997; Bradbury, 1997; Li et al., 2004). The record from Searles Lake indicates overflow around 21–24 ka and possibly younger, but a closed basin between ca. 24 ka and 44 ka (Smith, 1968).

There is no evidence from this study that the Owens River system reached Panamint Valley during OIS 4, and the faunal evidence from DH-1 core instead indicates a shallow groundwater-supported lake or wetlands. The weak OIS 4 lacustrine events preserved in Death Valley and Panamint Valley cores seem to be consistent with the magnitude of the OIS 4 event in the $\delta^{18}O$ sea-surface temperature record (SST) (Lea et al., 2000) and the normalized paleotemperature curve (PC1) proposed by Winograd et al. (2006) rather than the Devils Hole record (Winograd et al., 2006). The SST and PC1 paleotemperature curves show a cooling period at ca. 55–65 ka that was smaller in magnitude and duration than both OIS 2 and OIS 6.

Field relations (Gale, 1914b; Blackwelder, 1933; Smith, 1976; Smith et al., 1983), ostracode assemblages, and Sr isotope geochemistry (Stewart, 1998; Stewart et al., 2001) indicate a major influx of Owens River water to Panamint Valley during the Gale highstand. We infer from the AAR results that the spillway-limited lake that produced the Gale strandlines in Panamint Valley was present during OIS 6 and (or) older glacial intervals, but that discharge over the spillway has not occurred more recently. The arrival of Owens River water via Wingate Wash to Death Valley sometime during OIS 6 was inferred by Forester et al. (2005) from ostracode assemblages. Geochronologic methods (OSL/TL, ^{36}Cl, U-series) have indicated younger apparent ages for the highstand deposits; however, there is considerable scatter and no evidence from Death Valley and Panamint Valley cores to substantiate large OIS 4 lakes, or overflow of Owens River–type water into Death Valley at that time.

Extensive groundwater-supported wetlands or shallow lakes were present during OIS 4 based on faunal associations in the DH-1&1a core and an extrapolated sedimentation rate from the upper part of the core. Thus, Searles Lake or a basin upstream was likely the terminal lake for the Owens River system during OIS 4. The ostracode assemblages that lived during OIS 4 thrived on discharge from the deep regional groundwater aquifer, type 3 hydrochemistry, whereas the OIS 2 and OIS 6 assemblages indicate high alk/Ca ratios indicative of Owens River, type 2 water (Forester, 1999, 2001; Bradbury and Forester, 2002; Table 4). Ostracode and foraminiferal faunal assemblages suggest that the valley was used by Pacific marine avian migrants during OIS 2 and OIS 4. Ostracode assemblages suggest that the valley was used by Gulf of Mexico marine avian migrants during OIS 6.

Results from dating methods used in this study indicate that a fairly large lake may have occupied Panamint Valley during OIS 2. The lake highstand was at ~500–518 m elevation, at least 90–100 m lower than the spillway at Wingate Wash. Smith (1968) and Smith et al. (1983) earlier concluded that Searles Lake overflowed into Panamint Valley during OIS 2 between ca. 24 and 15.5 ka. The OIS 2 lake(s) in both the Lake Hill and Ballarat basins of Panamint Valley had Owens River–type chemistry, suggesting that they may have been hydrologically linked through the basin divide, which is presently open with respect to groundwater transport (Carranza, 1965).

OIS 2 Shorelines in Nearby Basins

Results from this study support the conclusion of Smith et al. (1983) that the Owens River system was flowing into Panamint Valley via Searles Lake during OIS 2 until ca. 15.5 ka. The ^{14}C ages on tufa from the OIS 2 highstand in Panamint Valley of ca. 22–26 ka are similar to OIS 2 ages from Owens Lake (Bacon et al., 2006). Lacustrine and vegetation records from Owens Valley (Koehler and Anderson, 1995; Bacon et al., 2006), Death Valley (Anderson and Wells, 2003), and Lake Mojave (Wells et al., 2003) indicate a brief drying and lake-lowering event between 20 and 18 ^{14}C ka and a return to LGM lake elevations from ca. 18 until 15 ^{14}C ka (Ore and Warren, 1971; Wells et al., 2003; Bacon et al., 2006). The OIS 2 tufa ages from the Ballarat basin may also record this event, with a similar drop in lake level around 19 ^{14}C ka (Fig. 11).

The timing of the lacustrine regression and wetlands succession documented in the Lake Hill basin is consistent with the age of well-known "black mat" deposits in the Mojave and Amargosa regions (Quade et al., 1998, 2003) and the age of an extreme drying event around 12,500 ^{14}C yr B.P. at Owens Lake (Benson et al., 1997; Bacon et al., 2006). A pronounced reduction in spring and wetland activity noted in the southern Great Basin and Amargosa areas around 9500–7000 ^{14}C yr B.P. (Quade et al., 2003) and around 9600 in Death Valley (Lowenstein et al., 1999), and a drop in lake level between around 8000 and 7000 ^{14}C yr B.P. in Owens Valley (Bacon et al., 2006) seem to have started at ca. 10–10.5 ka in the Lake Hill basin, Panamint Valley.

CONCLUSIONS

Surficial deposits of Pleistocene Lake Gale (Gale, 1914a, 1914b; Gale strandlines of Smith, 1976) between 317 and 610 m elevation, as well as core material of glacial and interstadial age, indicate that Panamint Valley was intermittently occupied by water from two fundamentally different sources: type 2 waters, characteristic of the Owens River system (cf. Forester, 1983, 1986, 1987, 1991; Stewart, 1998; Stewart et al., 2001), and type 3 waters, characteristic of a deep, thermally heated regional aquifer (Li et al., 1997). Mixing of these waters in Panamint Valley is a function of the timing and duration of spillover from the Owens River system during climatically controlled highstands (Smith, 1968; Smith et al., 1983; Stewart et al., 2001). The chemistry of the source waters is sufficiently unique to influence the ostracode assemblages (Forester, 1999, 2001; Forester et al., 2005) and is thus a relative indicator of the connectivity of the Owens River system to Panamint Valley (Stewart, 1998; Stewart et al., 2001).

Assuming that the ^{14}C ages on tufa represent the deposition or formation age of the tufa, a water body sufficiently large to occupy both the Lake Hill and Ballarat basins with Owens River–dominated water was present in Panamint Valley during OIS 2. Although the OIS 2 lake appears to have been ~180–200 m deep, it was not sufficiently large to spill into Death Valley. We conclude that Panamint Valley was occupied only by groundwater-supported wetlands and shallow lakes during OIS 4. Thus, it appears that the last time Panamint Valley spilled into Death Valley was most likely during OIS 6 or earlier, which is consistent with the presence of large lakes that have been extensively identified elsewhere in the Owens River system and Great Basin (Smith et al., 1983; Smith and Bischoff, 1997; Forester et al., 2005).

ACKNOWLEDGMENTS

We gratefully acknowledge Saxon Sharpe, Desert Research Institute, Tim Lowenstein, State University New York at Binghamton, and Jeff Pigati, U.S. Geological Survey (USGS), Tucson, for constructive and insightful reviews. We also thank Marith Reheis for thorough editing and many additional helpful comments. We also acknowledge lively discussions during the Friends of the Pleistocene field trips to Yucca Mountain (1997), Owens Valley (1998), Alvord Desert (1990), and Death Valley (2001) with many Quaternary geologists who pioneered lacustrine studies of this area. G.I. Smith shared much geological insight about the region and access to the archived DH-1&1a drill cores for sampling. Larry Benson provided information about the ^{14}C reservoir effect in nearby basins. We thank Kelly Conrad, USGS Denver, for processing the ostracode samples; Jordon Bright, Northern Arizona University, for picking organic concentrates for AMS ^{14}C analysis from DH-1; Laura Strickland, USGS Denver, for kindly identifying *Ruppia* sp. seeds (Wigeongrass) in DH-1 samples; and Steve Bacon, Desert Research Institute, for calibrating the conventional ^{14}C ages in Table 1.

REFERENCES CITED

Aitken, M.J., 1985, Thermoluminescence Dating: Academic Press, New York, 359 p.

Anderson, D.E., and Wells, S.G., 2003, Latest Pleistocene lake highstands in Death Valley, California, *in* Enzel, Y., Wells, S.G., and Lancaster, N., eds., Paleoenvironments and Paleohydrology of the Mojave and Southern Great Basin Deserts: Geological Society of America Special Paper 368, p. 115–128.

Bacon, S.N., Burke, R.M., Pezzopane, S.K., and Jayko, A.S., 2006, Latest Quaternary lake-levels of Owens Lake, Inyo County, California: Quaternary Research Reviews, v. 25, p. 1264–1282.

Bard, E.A., Hamelin, B., Tisnerat-Laborde, N., and Cabioch, G., 1998, Radiocarbon calibration by means of mass spectrometric ^{230}Th/ ^{234}U and ^{14}C ages of corals; an updated database including samples from Barbados: Mururoa and Tahiti: Radiocarbon, v. 40, p. 1085–1092.

Benson, L.V., Burdett, J.W., Lund, S.P., Kashgarian, M., and Mensing, S., 1997, Nearly synchronous climate change in the Northern Hemisphere during the last glacial termination: Nature, v. 388, p. 263–265, doi: 10.1038/40838.

Benson, L.V., Lund, S.P., Burdett, J.W., Kashgarian, M., Rose, P., Smoot, J.P., and Schwartz, M., 1998, Correlation of late-Pleistocene lake-level oscillations in Mono Lake, California, with North Atlantic climate events: Quaternary Research, v. 49, p. 1–10, doi: 10.1006/qres.1997.1940.

Benson, L.V., Liddicoat, J., Smoot, J.P., Sarna-Wojcicki, A.M., Negrini, R., and Lund, S., 2003a, Age of the Mono Lake excursion and associated tephra: Quaternary Science Reviews, v. 22, p. 135–140, doi: 10.1016/S0277-3791(02)00249-4.

Benson, L.V., Lund, S., Negrini, R., Linsley, B., and Zic, M., 2003b, Response of North American Great Basin lakes to Dansgaard-Oeschger oscillations: Quaternary Science Reviews, v. 22, p. 2239–2251, doi: 10.1016/S0277-3791(03)00210-5.

Bischoff, J.L., and Cummins, K., 2001, Wisconsin glaciation of the Sierra Nevada (79,000–15,000 yr B.P.) as recorded by rock flour in sediments of Owens Lake, California: Quaternary Research, v. 55, p. 14–24, doi: 10.1006/qres.2000.2183.

Blackwelder, E., 1933, Lake Manly, an extinct lake of Death Valley: Geographical Review, v. 23, p. 464–647, doi: 10.2307/209632.

Bradbury, J.P., 1997, A diatom-based paleohydrologic record of climate change for the past 800 k.y. from Owens Lake, California, *in* Smith, G.I., and Bischoff, J., eds., An 800,000-Year Paleoclimatic Record from Core OL-92, Owens Lake, Southeast California: Geological Society of America Special Paper 317, p. 99–112.

Bradbury, J.P., and Forester, R.M., 2002, Environment and paleolimnology of Owens Lake, California: A record of climate and hydrology for the past 50,000 years, *in* Hershler, R., Madsen, D.B., and Currey, D.R., eds., Great Basin Aquatic Systems History: Smithsonian Contributions to the Earth Sciences, v. 33, p. 145–174.

Campbell, M.R., 1902, Reconnaissance of the Borax Deposits of Death Valley and Mojave Desert: U.S. Geological Survey Bulletin B-200, 23 p.

Carranza, C., 1965, Surficial Geology of a Portion of South Panamint Valley, Inyo County, California [Master's thesis]: Amherst, University of Massachusetts, 225 p.

Carter, C., 1997, Ostracodes in Owens Lake core OL-92; alteration of saline and freshwater forms through time, *in* Smith, G.I., and Bischoff, J., eds., An 800,000-Year Paleoclimatic Record from Core OL-92, Owens Lake, Southeast California: Geological Society of America, Special Paper 317, p. 113–119.

Davis, E.L., 1970, Archeology of the north basin of Panamint Valley, Inyo County, California: Nevada State Museum Anthropological Papers, v. 15, p. 83–141.

Delorme, L.D., 1989, Methods in Quaternary Ecology. No. 7: Freshwater ostracodes: Geoscience Canada, v. 16, p. 85–90.

DePaolo, D.J., 1981, A neodymium and strontium isotopic study of the Mesozoic calc-alkaline granitic batholiths of the Sierra Nevada and Peninsular Ranges, California: Journal of Geophysical Research, v. 86, p. 10,470–10,488.

Domenick, M.A., Kistler, R.W., Dodge, F.C.W., and Tatsumoto, M., 1983, Nd and Sr isotopic study of crustal and mantle inclusions from the Sierra Nevada and implications for batholith petrogenesis: Geological Society of America Bulletin, v. 94, p. 713–719, doi: 10.1130/0016-7606(1983)94<713:NASISO>2.0.CO;2.

Elmore, D., Fulton, B.R., Clover, M.R., Marsden, J.R., Gove, H.E., Naylor, H., Purser, K.H., Kilius, L.R., Beukens, R.P., and Litherland, A.E., 1979, Analysis of ^{36}Cl in environmental water samples using an electrostatic accelerator: Nature, v. 277, p. 22–25, doi: 10.1038/277022a0.

Eugster, H.P., and Jones, B.F., 1979, Behavior of major solutes during closed-basin brine evolution: American Journal of Science, v. 279, p. 609–631.

Fitzpatrick, J.A., and Bischoff, J.L., 1993, Uranium-Series Dates on Sediments of the High Shoreline of Panamint Valley, California: U.S. Geological Survey Open-File Report 93-0232, 15 p.

Fitzpatrick, J.A., Bischoff, J.L., and Smith, G.I., 1993, Uranium-Series Analyses of Evaporites from the 1000-Foot PAN-3 Core, Panamint Valley, California: U.S. Geological Survey Open-File Report 93-558, 22 p.

Forester, R.M., 1983, Relationship of two lacustrine ostracode species to solute composition and salinity: Implication for paleohydrochemistry: Geology, v. 11, p. 435–438, doi: 10.1130/0091-7613(1983)11<435:ROTLOS>2.0.CO;2.

Forester, R.M., 1986, Determination of the dissolved anion composition of ancient lakes from fossil ostracodes: Geology, v. 14, p. 796–798, doi: 10.1130/0091-7613(1986)14<796:DOTDAC>2.0.CO;2.

Forester, R.M., 1987, Late Quaternary paleoclimate records from lacustrine ostracodes, *in* Ruddiman, W.F., and Wright, H.E., Jr., eds., North America and Adjacent Oceans during the Last Deglaciation: Boulder, Colorado, Geological Society of America, Geology of North America, v. K-2, p. 261–276.

Forester, R.M., 1991, Ostracode assemblages from springs in the Western United States: Implications for paleohydrology, *in* Williams, D.D., and Danks, H.V., eds., Arthropods of Springs, with Particular Reference to Canada: Memoirs of the Entomological Society of Canada, v. 155, p. 181–201.

Forester, R.M., 1999, Ostracodes as Indicators of Present and Past Hydrology in Death Valley: U.S. Geological Survey Open-File Report 99-153, p. 69–70.

Forester, R.M., 2001, An Ostracode Record of Holocene Climate Change from Owens Lake, California: U.S. Geological Survey Open-File Report 01-202, p. 7–8.

Forester, R.M., Lowenstein, T.K., and Spencer, R.J., 2005, An ostracode based paleolimnologic and paleohydrologic history of Death Valley; 200 to 0 ka: Geological Society of America Bulletin, v. 117, p. 1379–1386, doi: 10.1130/B25637.1.

Forman, S.L., and Pierson, J., 2002, Late Pleistocene luminescence chronology of loess deposition in the Missouri and Mississippi River valleys, United States: Palaeogeography, Palaeoclimatology, Palaeoecology, v. 186, p. 25–46, doi: 10.1016/S0031-0182(02)00440-6.

Gale, H.S., 1914a, Notes on the Quaternary Lakes of the Great Basin, with Special Reference to the Deposition of Potash and Other Salines: U.S. Geological Survey Bulletin 540, p. 399–475.

Gale, H.S., 1914b, Salines in the Owens, Searles, and Panamint Valleys, Southeastern California: U.S. Geological Survey Bulletin 580-L, p. 251–323.

Geyh, M.A., Schotterer, U., and Grosjean, M., 1998, Temporal changes of the ^{14}C reservoir effect in lakes, *in* Mook, W.G., and van der Plicht, J., eds., Proceedings of the 16th International Radiocarbon Conference, June 16–20, 1997, v. 40: Groningen, Netherlands, p. 921–931.

Gilbert, G.K., 1890, Lake Bonneville: U.S. Geological Survey Monograph 1, 309 p.

Gosse, J.C., and Phillips, F.M., 2001, Terrestrial in-situ cosmogenic nuclides: Theory and application: Quaternary Science Reviews, v. 20, p. 1475–1560, doi: 10.1016/S0277-3791(00)00171-2.

Groves, K.R., 1996, Geochemical and Isotopic Analysis of Pleistocene Basalts from the Southern Coso Volcanic Field, California [Master's thesis]: Chapel Hill, University of North Carolina, 84 p.

Hajdas, I., Bonani, G., Zimmerman, S.H., Mendelson, M., and Hemming, S., 2004, ^{14}C ages of ostracodes from Pleistocene lake sediments of the western Great Basin, USA; results of progressive acid leaching, *in* Beavan-Athfield, N., and Sparks, R.J., eds., Proceedings of the 18th International Radiocarbon Conference, September 1–5, 2003: Wellington, New Zealand, Radiocarbon, v. 46, p. 189–200.

Hall, W.E., and MacKevett, E.M., Jr., 1962, Geology and Ore Deposits of the Darwin Quadrangle, Inyo County, California: U.S. Geological Survey Professional Paper 368, 87 p.

Hanna, G.D., 1963, Some Pleistocene and Pliocene freshwater mollusca from California and Oregon: California Academy of Science Occasional Paper 43, 20 p.

Hershler, R., 1999, A systematic review of the *Hydrobiid* snails (Gastropoda: *Rissooidea*) of the Great Basin, western United States. Part II. Genera *Colli-*

gyrus, Eremopyrgus, *Fluminicola, Pristinicola,* and *Tryonia:* The Veliger, v. 42, p. 306–337.

Hershler, R., Liu, H., and Mulvey, M., 1999, Phylogenetic relationships within the aquatic snail genus Tryonia: Implications for biogeography of the North American Southwest: Molecular Phylogenetics and Evolution, v. 13, p. 377–391, doi: 10.1006/mpev.1999.0659.

Hubbs, C.L., Bien, G.S., and Suess, H.E., 1965, La Jolla natural radiocarbon measurements IV: Radiocarbon, v. 7, p. 66–117.

Jannik, N.O., Phillips, F.M., Smith, G.I., and Elmore, D., 1991, A ^{36}Cl chronology of lacustrine sedimentation in the Pleistocene Owens River system: Geological Society of America Bulletin, v. 103, p. 1146–1159, doi: 10.1130/0016-7606(1991)103<1146:ACCOLS>2.3.CO;2.

Jayko, A.S., 2005, Late Quaternary denudation rates, Death and Panamint Valleys, eastern California: Earth-Science Reviews, v. 73, p. 271–289, doi: 10.1016/j.earscirev.2005.04.009.

Jayko, A.S., 2008, Surficial Geology of the Darwin Hills $30' \times 60'$ Quadrangle, Inyo County, California: U.S. Geological Survey Map Series, scale 1:100,000.

Jayko, A.S., Forester, R.M., Sharpe, S.E., and Smith, G.I., 2001, The last pluvial highstand in Panamint Valley, southeast California: Eos (Transactions, American Geophysical Union), v. 88, p. 788.

Jayko, A.S., Forester, R.M., and Yount, J.C., 2002, Distribution and character of late Pleistocene lacustrine and spring deposits Panamint Valley, California: Geological Society of America Abstracts with Programs, v. 34, no. 6, p. 395.

Jones, B.F., 1966, Geochemical evolution of closed basin water in the western Great Basin, *in* Rau, J.L., ed., Second Symposium on Salt: Northern Ohio Geological Society, v. 1, p. 181–200.

Kaufman, D.S., 2000, Amino acid racemization in ostracodes, *in* Goodfriend, G., Collins, M., Fogel, M., Macko, S., and Wehmiller, J., eds., Perspectives in Amino Acid and Protein Geochemistry: New York, Oxford University Press, p. 145–160.

Kaufman, D.S., 2003a, Amino acid paleothermometry of Quaternary ostracodes from the Bonneville Basin, Utah: Quaternary Science Reviews, v. 22, p. 899–914, doi: 10.1016/S0277-3791(03)00006-4.

Kaufman, D.S., 2003b, Dating deep-lake sediments by using amino acid racemization in fossil ostracodes: Geology, v. 31, p. 1049–1052, doi: 10.1130/ G20004.1.

Kaufman, D.S., and Manley, W.F., 1998, A new procedure for determining enantiomeric (D/L) amino acid ratios in fossils using reverse phase liquid chromatography: Quaternary Science Reviews, v. 17, p. 987–1000, doi: 10.1016/S0277-3791(97)00086-3.

Kaufman, D.S., O'Brien, G., Mead, J.I., Bright, J., and Umhoefer, P., 2002, Late Quaternary spring-fed deposits of the Grand Canyon and their implication for deep lava-dammed lakes: Quaternary Research, v. 58, p. 329–340, doi: 10.1006/qres.2002.2375.

Kistler, R.W., and Peterman, Z.E., 1973, Variations in Sr, Rb, K, Na, and initial Sr^{87}/Sr^{86} in Mesozoic granitic rocks and intruded wall rocks in central California: Geological Society of America Bulletin, v. 84, p. 3489–3512, doi: 10.1130/0016-7606(1973)84<3489:VISRKN>2.0.CO;2.

Kistler, R.W., and Peterman, Z.E., 1978, Reconstruction of crustal blocks of California on the basis of initial strontium isotopic compositions of Mesozoic granitic rocks: U.S. Geological Survey Professional Paper 1071, 17 p.

Koehler, P.A., and Anderson, R.S., 1995, Thirty thousand years of vegetation changes in the Alabama Hills, Owens Valley, California: Quaternary Research, v. 43, p. 238–248, doi: 10.1006/qres.1995.1024.

Kunkel, F., 1962, Preliminary Map Showing Valley-Fill Areas and Source, Occurrence, and Movement of Ground Water in the Western Part of the Mojave Desert Region, California: U.S. Geological Survey, Hydrologic Investigations Atlas HA-0031, scale 1:316,800.

Laabs, B.J.C., and Kaufman, D.S., 2003, Quaternary highstands in Bear Lake Valley, Utah and Idaho: Geological Society of America Bulletin, v. 115, p. 463–478, doi: 10.1130/0016-7606(2003)115<0463:QHIBLV>2.0.CO;2.

Lal, D., 1991, Cosmic ray labeling of erosion surfaces; in situ nuclide production rates and erosion models: Earth and Planetary Science Letters, v. 104, p. 424–439.

Lang, A., 1994, Infrared stimulated luminescence dating of Holocene reworked silty sediments: Quaternary Science Reviews, v. 13, p. 525–528, doi: 10.1016/0277-3791(94)90071-X.

Lea, D.W., Pak, D.K., and Spero, H.J., 2000, Climate impact of late Quaternary equatorial Pacific sea surface temperature variations: Science, v. 289, p. 1719–1724, doi: 10.1126/science.289.5485.1719.

Li, H., Bischoff, J.L., Ku, T., and Zhu, Z., 2004, Climate and hydrology of the last interglaciation (MIS 5) in Owens Basin, California: Isotopic and geochemical evidence from core OL-92: Quaternary Science Reviews, v. 23, p. 49–63, doi: 10.1016/S0277-3791(03)00215-4.

Li, J., Lowenstein, T.K., and Blackburn, I.R., 1997, Responses of evaporite mineralogy to inflow water sources and climate during the past 100 k.y. in Death Valley, California: Geological Society of America Bulletin, v. 109, p. 1361–1371, doi: 10.1130/0016-7606(1997)109<1361:ROEMTI>2.3.CO;2.

Lowenstein, T.K., Li, J., Brown, C., Roberts, S.M., Ku, T.-L., Luo, S., and Yang, W., 1999, 200 k.y. paleoclimate record from Death Valley salt core: Geology, v. 27, p. 3–6, doi: 10.1130/0091-7613(1999)027<0003:KYPRFD>2.3.CO;2.

McConnaughey, T., 1991, Calcification of Chara corallina: CO_2 hydroxylation generates protons for bicarbonate assimilation: Limnology and Oceanography, v. 36, p. 618–628.

McConnell, V.S., 1994, Applying Sr isotope geochemistry to interpreting the history of the Long Valley caldera, California: Eos (Transactions, American Geophysical Union), v. 75, p. 733.

Miller, G.H., and Brigham-Grette, J., 1989, Amino acid geochronology–resolution and precision in carbonate fossils: Quaternary International, v. 1, p. 111–128, doi: 10.1016/1040-6182(89)90011-6.

Ore, H.T., and Warren, C.N., 1971, Late Pleistocene–early Holocene geomorphic history of Lake Mojave, California: Geological Society of America Bulletin, v. 82, p. 2553–2562, doi: 10.1130/0016-7606(1971)82[2553:LPHGHO]2.0.CO;2.

Phillips, F.M., and Plummer, M.A., 1996, CHLOE: A program for interpreting in-situ cosmogenic nuclide data for surface exposure dating and erosion studies, *in* Jull, A.J.T., ed., 7th International Conference on Accelerator Mass Spectrometry: Radiocarbon Abstracts, v. 38, p. 98–99.

Phillips, F.M., and Zreda, M.G., 1999, Chlorine-36 Ages of Pluvial Shoreline Features in the Death Valley/Panamint Valley Area: U.S. Geological Survey Open-File Report 99-153, p. 69–70.

Phillips, F.M., Stone, W.D., and Fabryka-Martin, J.T., 2001, An improved approach to calculating low-energy cosmic-ray neutron fluxes near the land/atmosphere interface: Chemical Geology, v. 175, p. 689–701, doi: 10.1016/S0009-2541(00)00329-6.

Prescott, J.R., and Hutton, J.T., 1994, Cosmic ray contributions to dose rates for luminescence and ESR dating: Large depths and long-term time variations: Radiation Measurements, v. 23, p. 497–500, doi: 10.1016/1350-4487(94)90086-8.

Pretti, V.A., and Stewart, B.W., 2002, Solute sources and chemical weathering in the Owens Lake watershed, eastern California: Source Water Resources Research, v. 38, 18 p.

Quade, J., Forester, R.M., Pratt, W.L., and Carter, C., 1998, Black mats, spring fed-streams and late-glacial age recharge in the southern Great Basin: Quaternary Research, v. 49, p. 129–148, doi: 10.1006/qres.1997.1959.

Quade, J., Forester, R.M., and Whelan, J.F., 2003, Late Quaternary paleohydrologic and paleotemperature change in southern Nevada, *in* Enzel, Y., Wells, S.G., and Lancaster, N., eds., Paleoenvironments and Paleohydrology of the Mojave and Southern Great Basin Deserts: Geological Society of America Special Paper 368, p. 165–188.

Reheis, M.C., and Sawyer, T.L., 1997, Late Cenozoic history and slip rates of the Fish Lake Valley, Emigrant Peak and Deep Springs fault zones, Nevada and California: Geological Society of America Bulletin, v. 109, p. 280–299, doi: 10.1130/0016-7606(1997)109<0280:LCHASR>2.3.CO;2.

Reimer, P.J., Baillie, M.G., Bard, E., Bayliss, A., Beck, J.W., Bertrand, C.J.H., Blackwell, P.G., Buck, C.E., Burr, G.S., Cutler, K.B., Damon, P.E., Edwards, R.L., Fairbanks, R.G., Friedrich, M., Guilderson, T.P., Hogg, A.G., Hughen, K.A., Kromer, B., McCormac, G., Manning, S., Ramsey, C.B., Reimer, R.W., Remmele, S., Southon, J.R., Stuiver, M., Talamo, S., Taylor, F.W., van der Plicht, J., and Weyhenmeyer, C.E., 2004, IntCal04 terrestrial radiocarbon age calibration, 0–26 cal kyr B.P.: Radiocarbon, v. 46, p. 1029–1058.

Richardson, C.A., McDonald, E.V., and Busacca, A.J., 1997, Luminescence dating of loess from the northwest United States: Quaternary Science Reviews, v. 16, p. 403–415, doi: 10.1016/S0277-3791(96)00111-4.

Russell, I.C., 1885, Geological History of Lake Lahontan, A Quaternary lake of Northwestern Nevada: U.S. Geological Survey Monograph XI, 288 p.

Singhvi, A.K., Sharma, Y.P., and Agrawal, D.P., 1982, Thermo-luminescence dating of sand dunes in Rajasthan, India: Nature, v. 295, p. 313–315, doi: 10.1038/295313a0.

Smith, A.J., 1993, Lacustrine ostracodes as hydrochemical indicators in lakes of the north-central United States: Journal of Paleolimnology, v. 8, p. 121–134, doi: 10.1007/BF00119785.

Smith, G.I., 1968, Late Quaternary geologic and climatic history of Searles Lake southeastern California, *in* Morrison, R.B., and Wright, H.E., Jr., eds., Means of Correlation of Quaternary Successions, Volume 8: Salt Lake City, University of Utah Press, p. 293–310.

Smith, G.I., and Bischoff, J.L., eds., 1997, An 800,000-Year Paleoclimatic Record from Core OL-92, Owens Lake, Southeast California: Geological Society of America Special Paper 317, 165 p.

Smith, G.I., and Pratt, W.P., 1957, Core Logs from Owens, China, Searles, and Panamint Valleys, California: U.S. Geological Survey Bulletin 1045-A, 62 p.

Smith, G.I., Barczak, V.J., Moulton, G.F., and Liddicoat, J.C., 1983, Core KM-3, a Surface-to-Bedrock Record of Late Cenozoic Sedimentation in Searles Valley, California: U.S. Geological Survey Professional Paper 1256, 24 p.

Smith, R.L., Roof, S.R., and Savoy, L.E., 1998, Interpreting Pleistocene history of Panamint Valley, southeastern California, using gastropod shells: Geological Society of America Abstracts with Programs, v. 30, no. 7, p. A-284.

Smith, R.S.U., 1976, Late-Quaternary Fluvial and Tectonic History of Panamint Valley, Inyo and San Bernardino Counties, California [Ph.D. thesis]: Pasadena, California Institute of Technology, 295 p.

Smith, R.S.U., 1978, Pluvial History of Panamint Valley, California: Pacific Cell, Friends of the Pleistocene, Guidebook, 36 p.

Steinkampf, W.C., and Werrell, W.L., 2001, Ground-water flow to Death Valley, as inferred from the chemistry and geohydrology of selected springs in Death Valley National Park, California and Nevada: U.S. Geological Survey Water-Resources Investigations Report 98-4114, 37 p.

Stewart, B.W., 1998, Quaternary weathering processes and climate change in the Sierra Nevada and western Great Basin; radiogenic isotope results from the Owens River system: Geological Society of America Abstracts with Programs, v. 30, no. 7, p. A-66.

Stewart, B., Roof, S., Boulanger, J.R., and Lowenstein, T.K., 2001, Connectivity of Owens River system paleo-lakes during Quaternary glacial periods: The strontium isotope record: Eos (Transactions, American Geophysical Union), v. 88, p. 788.

Stone, J.O.H., Evans, J.M., Fifield, L.K., Allan, G.L., and Cresswell, R.G., 1998, Cosmogenic chlorine-36 production in calcite by muons: Geochimica et Cosmochimica Acta, v. 62, p. 433–454, doi: 10.1016/S0016-7037(97)00369-4.

Stuiver, M., 1964, Carbon isotopic distribution and correlated chronology of Searles Lake sediments: American Journal of Science, v. 262, p. 377–392.

Stuiver, M., and Polach, H.A., 1977, Discussion: Reporting of ^{14}C dating: Radiocarbon, v. 19, p. 355–363.

Stuiver, M., and Reimer, P.J., 1993, Extended ^{14}C database and revised CALIB 3.0 ^{14}C age calibration program: Radiocarbon, v. 35, p. 215–230.

Taylor, D.W., 1986, Fossil molluscs from the Lake Hill archeological site, Panamint Valley, southeastern California: Contributions of the Great Basin Foundation, v. 2, p. 42–53.

Vogel, M., Jayko, A.S., Wooden, J., and Smith, R.S.U., 2002, Quaternary exhumation rate, central Panamint Range, California, from U-Pb zircon ages: Geological Society of America Abstracts with Programs, v. 34, no. 6, p. 249.

Wasserburg, G.J., Albee, J., and Lanphere, M., 1964, Migration of radiogenic strontium during metamorphism: Journal of Geophysical Research, v. 69, p. 4395–4401.

Wehmiller, J.F., 1984, Interlaboratory comparison of amino acid enantiomeric ratios in fossil Pleistocene mollusks: Quaternary Research, v. 22, p. 109–120, doi: 10.1016/0033-5894(84)90010-3.

Wehmiller, J.F., and Miller, G.H., 2000, Aminostratigraphic dating methods in Quaternary geology, *in* Noller, J.S., Sowers, J.M., and Lettis, W.R., eds., Quaternary Geochronology: Methods and Applications: Washington, D.C., American Geophysical Union, Reference Shelf, v. 4, p. 187–222.

Wells, S.G., Brown, W.J., Enzel, Y., Anderson, R.Y., and McFadden, L.D., 2003, Late Quaternary geology and paleohydrology of pluvial Lake Mojave, southern California, *in* Enzel, Y., Wells, S.G., and Lancaster, N., eds., Paleoenvironments and Paleohydrology of the Mojave and Southern Great Basin Deserts: Geological Society of America Special Paper 368, p. 79–114.

Winograd, I.J., Landwehr, J.M., Coplen, T.B., Sharp, W.D., Riggs, A.C., Ludwig, K.R., and Kolesar, P.T., 2006, Devils Hole, Nevada, $\delta^{18}O$ record extended to the mid-Holocene: Quaternary Research, v. 66, p. 202–212.

Wornardt, W.W., 1964, Pleistocene Diatoms from Mono and Panamint Lake Basins, California: California Academy of Science Occasional Paper 46, 27 p.

Zreda, M.G., 1994, Development and Calibration of the Cosmogenic ^{36}Cl Surface Exposure Dating Method and Its Application to the Chronology of Late Quaternary Glaciations [Ph.D. thesis]: Socorro, New Mexico Institute of Mining and Technology, 318 p.

Manuscript Accedpted by the Society 17 July 2007

Printed in the USA